Journal of Biomolecular Structure and Dynamics

ISSN: (Print) (Online) Journal homepage: https://www.tandfonline.com/loi/tbsd20

A combined *in vitro–in silico* approach for the discovery of novel endogenous enzymatic and ctDNA sequence of bioactive molecules from aerial and root parts of *Centaurea sulphurea* as antioxidant's agents

Benhamidat Lyna, Mesli Fouzia, Bensaid Okkacha, Mohammed El Amine Dib & Alain Muselli

To cite this article: Benhamidat Lyna, Mesli Fouzia, Bensaid Okkacha, Mohammed El Amine Dib & Alain Muselli (2022): A combined *in vitro–in silico* approach for the discovery of novel endogenous enzymatic and ctDNA sequence of bioactive molecules from aerial and root parts of *Centaurea sulphurea* as antioxidant's agents, Journal of Biomolecular Structure and Dynamics, DOI: 10.1080/07391102.2022.2090438

To link to this article: https://doi.org/10.1080/07391102.2022.2090438

JOURNAL OF BIOMOLECULAR STRUCTURE AND DYNAMICS
https://doi.org/10.1080/07391102.2022.2090438

Taylor & Francis
Taylor & Francis Group

A combined *in vitro–in silico* approach for the discovery of novel endogenous enzymatic and ctDNA sequence of bioactive molecules from aerial and root parts of *Centaurea sulphurea* as antioxidant's agents

Benhamidat Lyna[a], Mesli Fouzia[a], Bensaid Okkacha[a], Mohammed El Amine Dib[a] and Alain Muselli[b]

[a]Laboratoire des Substances Naturelles & Bioactives (LASNABIO), Département de Chimie, Faculté des Sciences, Université Abou BekrBelkaıd, Tlemcen, Algeria; [b]Laboratoire Chimie des Produits Naturels, Université de Corse, UMR CNRS 6134, Corté, France

Communicated by Ramaswamy H. Sarma

ABSTRACT

The excess free radicals not neutralized by the antioxidant defenses damage the essential macromolecules of our cells, causing abnormalities in the expression of genes and membrane receptors, cell proliferation or death, immune disorders, mutagenesis, deposits of proteins or lipofuschin in tissues. The first objective of this study was to elucidate the composition of the essential oil of the aerial and root part of *Centaurea sulphurea* during beginning of the vegetative cycle (March), beginning of the flowering stage (April) and full bloom (May/June) using GC/FID and GC/MS. The second aim was to describe the antioxidant activity using three methods (2,2-diphenyl-1-picrylhydrazyl (DPPH), ferric-reducing antioxidant power (FRAP), β-carotene bleaching assay) and bioinformatical study of ct*DNA* sequence and three endogenous enzymes inhibition. The essential oils obtained from the root during the full bloom period consisted mainly of caryophyllene oxide, aplotaxene and (Z)-phytol. While, the aerial parts were dominated by caryophyllene oxide, verridiflorol and humulene epoxide II. The results showed that essential oil presented an excellent antioxidant activity with IC_{50} values of 2.06 g/L and 1.29 g/L, for aerial and root parts, compared to butylated hydroxyltoluene (BHT) and Ethylenediaminetetraacetic acid (EDTA) controls and the nicotinamide adenine dinucleotide phosphate (NADPH) co-crystallized inhibitor. The results of the molecular docking revealed that (Z)-phytol (Ligand 39) has an affinity to interact with ctDNA sequence, and three targets *Endogenous enzymes*. The molecular dynamics study was conducted for the best inhibitors (Z)-phytol. A few key residues were identified at the binding site of receptors. The in-silico assessment of the ADME properties and BOILED-Egg plot reveals that compound (Z)-phytol (L39) is permeable to the blood brain barrier and have high lipophilicity and high coefficient of skin permeability in the intestines with good bioavailability. The ADMET analysis also showed that this oxygenated diterpene is safer to replace the synthetic drugs with side effects. Further testing is needed to assess its effectiveness in reducing oxidative stress for use in the pharmaceutical industry.

ARTICLE HISTORY
Received 8 September 2021
Accepted 11 June 2022

KEYWORDS
C. sulphurea; antioxidant; *in silico*; ct*DNA* binding; MOE (Molecular Operating Environment)

1. Introduction

Antioxidants have been widely used as additives to help maintain quality and increase the shelf life of the product. Also, antioxidants have an important role in the prevention of various diseases because they suppress active oxygen and lipid peroxidation (Noguchi & Niki, 1999). The antioxidant capacity of essential oils can be evaluated either *in vivo*, on living organisms or *in-vitro*, by using methods that involve the mixture of oxidant species with a sample that contains antioxidants capable of inhibiting the generation of free radicals (Alam et al., 2013). The latter can act under different mechanisms such as free radical decomposition, free radical scavenging and to chelate ferrous ions (Çam et al., 2009). Synthetic antioxidants, such as butylated hydroxyanisole (BHA) and butylated hydroxyltoluene (BHT), have been widely used, but due to their undesirable effect, the naturally occurring antioxidants are highly desirable (Rodil et al., 2012). The *Centaurea* genus presents a great therapeutic interest. This genus belonging to the largest and important genera of Asteraceae family, it accounts for about more than five hundred species distributed all over the world (Trease et al., 1983). Forty-five species are cultivated in Algeria according to Quezel and Santa (Francisco et al., 1995). Among them, *C. sulphurea* which is an annual herbaceous species. Indeed, several phytochemical and pharmacological studies have shown its richness in natural bioactive substances. Many *Centaurea* species were used in traditional medicine to treat various diseases, such as diabetes, malaria, hemorrhoids, abscesses and colds (Kargı oğlu et al., 2010). Similarly, it has been beneficial in the treatment of cancer and microbial infections (Kumarasamy et al., 2003; Panagouleas et al., 2003). The flowering tops of *C. sulphurea*

CONTACT Mesli Fouzia meslifouzia2018@gmail.com; Mohammed El Amine Dib a_dibdz@yahoo.fr Laboratoire des Substances Naturelles & Bioactives (LASNABIO), Département de Chimie, Faculté des Sciences, Université Abou BekrBelkaıd, Tlemcen, Algeria

Supplemental data for this article can be accessed online at https://doi.org/10.1080/07391102.2022.2090438.

are used in decoction against palpitations (Secilla et al., 2012). Previous phytochemical work of this species has shown that chloroform extracts of the aerial part were rich in sesquiterpene lactones such as sulfureidine (Lakhal et al., 2010) and flavonoid aglycones such cirsilineol, jaceosidin, 3-O-methyl-eupatorin, eptin and eupatilin (Kabouche et al., 2011). The endogenous enzymatic antioxidant defense system such as superoxide dismutase (SOD), catalase (CAT), glutathione peroxidase (GPxs), play an important role in homeostatic redox balance (Eddaikra et al., 2021). These defense systems are important and indispensable in the entire defense strategy of antioxidants, especially in reference to super oxide anion radical ($^{*}O_2$) (Ighodaro et al., 2018).

The computational technique known as "docking" can predict the binding of drug–target complex, as well as the conformation of the ligand upon binding to a protein target. It makes it possible to represent, interpret and predict biomolecular structures and functions (Mesli et al., 2013).

To the best of our knowledge, no studies have investigated the chemical composition and the biological activities of *C. sulphurea* essential oil. The main interest of this study was to study first the chemical composition of essential oil of *C. sulphurea* during the three developmental stages and the investigation of their antioxidant properties. The second study was to try to elucidate how the molecules of this oil interact with three powerful endogenous enzyme (catalase (CAT), superoxide dismutase (SODs), glutathione peroxidase (GPx)) and c*tDNA* sequence. Knowing that these endogens are active in endothelial cells, cytoplasm and mitochondrial intermembrane matrix (Oury et al., 1996).

The previous studies have shown that the catalase activation with a natural antioxidant component, which doesn't have toxicity, can provide useful results in the health field (Najjar et al., 2017). Also, other researchers have reported that catalase inhibition by wogonin led to H_2O_2 accumulation and cytotoxicity in cancer cells through H_2O_2-mediated NF-κB suppression and apoptosis activation (Pal et al., 2014; Yang et al., 2011). In this research, the plat form package MOE (Molecular Operating Environment) was used to study the modeling applications between all compounds of *C. sulphurea* essential oil and the catalase enzyme. After that, the compounds that achieved both good score in docking with catalase were docked with two endogenous enzymes: Superoxide Dismutase (Manjula et al., 2018), Glutathione Peroxidase (Tars et al., 2010) enzymes and *Ct-DNA* sequence (CGCGAATTCGCG)2 dodecamer (Drew et al., 1980), in order to validate the best interactions with the nucleotides and their affinities.

The main interest was to develop unique potential inhibitors of endogenous enzymatic (catalase (CAT), superoxide dismutase (SODs), glutathione peroxidase (GPx) and *ctDNA* sequence, to combat free radicals and protect the body from the damage caused by them. The docking studies predicted that the constituent molecules of the aerial and root parts of essential oil of *C. sulphure* possess more capability as inhibitors as compared to established drugs in the pharmaceutical industry. Further, five designed compounds were filtered through Lipinski's rule of five, along with ADMET risk parameters assessments. Finally, the top hit compound Z-phytol was analyzed by system pharmacology approaches.

2. Material and methods

2.1. Experimental procedures

2.1.1. Chemicals used in the study

Solvents and reagents used were 2,2-diphenyl-1-picrylhydrazyl (DPPH) and 2,2′-azino-bis(3-ethylbenzothiazoline-6-sulfonic acid (ABTS), ethanol, methanol, potassium persulfate, iron chloride, ferrozine, BHT, EDTA, Quercetin and anhydrous sodium sulphate were purchased from Sigma (Sigma–Aldrich). In this study, we used analytical grade chemicals.

2.1.2. Plant material and extraction of essential oil

The plant materials of *C. sulphurea* were collected in the Zarifet forestwit latitude: 1°19′08″O; longitude: 34°52′20″N; altitude: 990 m) about 10 km from Tlemcen (Algeria). The essential oils of the aerial and root parts used for the study were collected at the beginning of April (Vegetative stage), at mid-May (Floral budding stage) and at the end of June (Flowering stage). The plant was identified by the botanist BABA Ali from the Department of Agronomy of the University of Tlemcen (Algeria), where a voucher specimen of the plant has been deposited in the Herbarium. Plant materials were air-dried at room temperature and submitted to hydro-distillation for 4 hours using a Clevenger apparatus according to the procedure described in the European Pharmacopeia (Conseil de l'Europe, 1996). The essential oils were treated with anhydrous sodium sulphate (Na_2SO_4) and stored in a sealed tube at −4 °C until further used for chemical analysis and antioxidant activity.

2.1.3. Identification of the oil components

2.1.3.1. Gas chromatography. The gas chromatography (GC) analysis was carried out using Clarus 500-Perkin-Elmer Auto system apparatus (Waltham, Massachusetts, USA) equipped by two flame ionization detectors (FID), with fused capillary columns (film thickness 0.25 μm;50 m × 0.22 mm I. D), BP-1 (polymethyl-siloxane) and BP-20 (polyethylene glycol); carrier gas, helium; linear velocity, 0.8 mL/min (Bekhechi et al., 2010). The oven temperature was fixed from 60 °C to 220 °C at 2 °C/min and then held isotherm (20 min) (Bereksi et al., 2018), injector temperature was 250 °C (injection mode: split 1/60); detector temperature 250 °C. The relative proportions of the essential oil constituents were expressed as percentages obtained by peak area normalization, without using correction factors, as described previously (Medbouhi et al., 2018).

2.1.3.2. Gas chromatography/mass spectrometry (GC/MS). Essential oils were analyzed with a Perkin ElmerTurbo-Mass quadrupole analyzer, coupled to a Perkin Elmer Auto system XL (France), equipped with two fused-silica capillary columns and operated with the same gas chromatography conditions

described above, except for a split of 1/80. Under the following conditions, EI mass spectra were acquired: Ion source temp. 150 °C, energy ionization 70 eV, mass range 35–350 Da (scan time: 1 s) (Zatla et al., 2017).

2.1.4. Component identification and quantification

Quantification and identification of the components were made (i) through the comparison of their GC retention indices (RI) on nonpolar and polar columns, determined relative to the retention time of a series of n-alkanes with linear interpolation, with those of authentic compounds or literature data (Bouyanzer et al., 2006; Jennings et al., 1980; König et al., 2004) and (ii) also through computer matching with commercial mass spectral libraries (National Institute of Standards and Technology, 1999) and comparison of spectra with those of in-library of laboratory of chemistry of natural products, University of Corsica (France). Component quantification was carried out using peak normalization % abundances calculated by integrating FID response factors relative to tridecane (0.7 g/100 g), used as an internal standard.

2.1.5. Antioxidant assays

2.1.5.1. DPPH free radical scavenging assay. The essential oil from the **flowering stage (June)** was used for the evaluation of antioxidant activity. Radical scavenging activity of essential oil was measured by the standard method and determined by using spectrophotometer. A volume of 1000 μl of various concentrations of oil ranging from (0.2–15 g/L) were prepared in ethanol and added 1 mL of 0.2 mM DPPH solution freshly prepared. After 30 min of incubation at 37 °C in the dark, the anti DPPH activity was measured by recording the absorbance at 517 nm against blank and standard (BHT). The percentage inhibition activity was calculated by the following equation (Dhami et al., 2018).

$$\text{DPPH scavenging effect\%} = \frac{(\text{Acontrol} - \text{Asample})}{\text{Acontrol}} \times 100 \quad (1)$$

where $A_{control}$ is absorbance of DPPH radical (without the test sample), and A_{sample} is the absorbance of DPPH radical with the oil samples of various concentrations. The IC_{50} (Half-maximal inhibitory concentration) was calculated graphically by the linear regression formula of the inhibition percentages as a function of different concentrations of the sample tested (Belabbes et al., 2017).

2.1.5.2. Metal chelating activity. The metal chelating assay by oils was examined by spectrophotometry method based on ability of essential oil to chelate transition metal ions Fe^{2+} by measuring the absorbance of iron-ferrozine complex formed at 562 nm (Kumar et al., 2012; Parki et al., 2017). In brief 100 μl of (0.6 mM) $FeCl_2$, 100 μl of 5 mM ferrozine and 900 μl mL of methanol were added to various concentrations of tested sample (0.2–15 mg/mL). The solutions were mixed thoroughly and incubated for 10 min (Dhami et al., 2018). The absorbance of test sample was measured in a UV spectrophotometer at 562 nm. All the readings were recorded in duplicate; EDTA (0.01 mM) was used as the standard. The metal-chelating activity of tested samples, expressed as percentage was calculated by using the following formula (Dhami et al., 2018).

$$\text{Chelating activity \%} = \frac{(\text{control} - \text{sample})}{\text{control}} \times 100 \quad (2)$$

The IC_{50} was calculated graphically by the linear regression formula of the inhibition percentages as a function of different concentrations of the sample tested.

2.1.5.3. β-carotene bleaching assay. The ability of *C. sulphurea* essential oils to protect lipid peroxidation was assessed by using the β-carotene bleaching test (Sangwan et al., 2001) this method is commonly used because β-carotene is an important physiological compound however it shows a strong biological activity (Kim et al., 2004). BHT was the positive control. Briefly, a mixture of β-carotene, Linoleic acid, and Tween 40 was prepared. The solvent was evaporated entirely by using a rotary evaporator. 100 mL of distilled water saturated with oxygen was added and shaken vigorously to form an emulsion. Then, 2.5 mL of the obtained emulsion was transferred into test tubes with 3.5 mL sample at different concentrations. The reaction mixture was maintained at 50 °C for 120 min, and the absorbance was measured at 470 nm using spectrophotometer against a blank consisting of an emulsion without β-carotene (Stankovic et al., 2020). The β-carotene bleaching assay was calculated as follows (Stankovic et al., 2020):

$$\beta - \text{carotene activity \%} = \frac{(\text{As}(120) - \text{AC}(120)}{(\text{AC}(0) - \text{A C}(120))} \times 100 \quad (3)$$

where $A_{s(120)}$ is the absorbance of the sample at t = 120 min, $A_{C(120)}$ is the absorbance of the control at t = 120 min, and $A_{C(0)}$ is the absorbance of the control at t = 0 min. The IC_{50} was calculated graphically by the linear regression formula of the inhibition percentages as a function of different concentrations of the sample tested.

2.2. Theoretical background and computational details

2.2.1. Preparation and optimization of both enzyme and inhibitors

In this study, the structures of all compounds were downloaded from PubChem database (https://pubchem.ncbi.nlm.nih.gov). The 3D structures of all compounds were pre-optimized by means of the Molecular Mechanics using Force Field MM+. After that, the resulted minimized structures were further refined using the semi-empirical method (AM1) (Stewart et al., 2007). All methods are implemented in Hyperchem 8.0.8 software (HyperChem v8, 2009). At the end, the database was created in which all the compounds were converted into their 3D structures and this database was used as an input file in MOE-docking. Both crystallographic structures of the human catalase (PDB ID: 1dgb Resolution = 2.20 Å) as can be seen from Figure 1, R-Value Free 0.227 (Putnam et al., 2000) and Ct-DNA sequenced (CGCGAATTCGCG)2 dodecamer (PDB ID: 1BNA; Resolution = 1.90 Å), R-Value Free 0.178 (Drew et al.,

1980) (were retrieved from the Protein Data Bank (PDB) (PDB; http://www.rcsb.org/pdb/home/home.do). In general, the protein structure with a resolution between 1.5 and 2.5 Å have an excellent quality for further studies (Clément & Slenzka, 2006; Didierjean & Tête-Favier, 2016), whereas, the resolution value of catalase and B-DNA belongs to this interval. Receptor (DNA) and ligand (the complex) files were prepared using platform package MOE (Molecular Operating Environment). The complex was enclosed in a box with the number of grid points in $x \times y \times z$ directions ($122 \times 72 \times 6$), and a grid spacing of 0.375 Å. All other parameters were default settings. For each of the docking cases, the lowest energy docked conformation, according to the package MOE (Molecular Operating Environment (MOE), 2013) scoring function, was selected as the binding mode.

2.2.2. Molecular docking

In this research, the platform package MOE (Molecular Operating Environment) was used to study the modeling applications between all compounds and the catalase enzyme. After that, the compounds that achieved good score in docking with catalase were docked to two Endogenous enzymes: Superoxide Dismutase (PDB ID: **5ytu**) **(**Manjula et al., 2018), Glutathione Peroxidase (PDB ID: **2vcv**) (Tars et al., 2010) enzymes and *Ct-DNA* sequence (CGCGAATTCGCG)2 dodecamer (PDB ID: **1BNA**) (Drew et al., 1980), in order to validate the best interactions with the nucleotides and their affinities. During the docking process the ligand was considered structurally rigid while the target was set as completely flexible. The wash setting was applied at pH6.0 and 300 K, hydrogen atoms were added, and protonation 3D were assigned. The minimum energy configuration was performed using the MMFF94x force field. OPLS-AA force field was used with conjugant gradient method (Jorgensen et al., 1996). To assign atom type and partial charges in receptor structure. The number of interactions varies between (0, n) where n is 10, the cut-off for coulomb interaction and Van der Waals interactions was 30 Å with the ability to study the hydrogen-electrostatic in the total active site of catalase was optimized and the results were discussed. Also, we followed the same protocol of Molecular docking simulation which is used in our previous studies (Chenafa et al., 2021; Daoud et al., 2018). The following default parameters were used: Placement: Triangle Matcher; Rescoring 1: London dG. The London dG scoring function was employed to estimate the lowest score energy of the complex for the best pose of the compounds tested. All simulations were run by using all explicit solvation models using TIP3P water. After that, the RMSD value was used to compare the differences between the atomic distances of the docked poses and the ligand molecule of reference pose (NADPH), where a threshold of 2.0 Å corresponding to the better solution (Cross et al., 2009). In the end, the binding energy between ligands and target catalase was calculated using molecular mechanics (MOE, 2013) and based on molecular mechanics (Halgren, 1996, 1999). The results of the top scoring complexes in the active site were selected for the further molecular dynamics simulation study.

Table 1. Plant material, vegetative cycle and oil yields of *C. sulphurea*.

		Essential oilyield (%)		
Month	Stage	Aerial part	Root part	Temperature (°C)
April	Vegetative stage	0.05	0.15	13
May	Floral budding stage	0.16	0.29	25
June	Flowering stage	0.25	0.38	36

2.2.3. Molecular dynamics simulation, ADMET, cytochromes P450 and pharmacophore mapping

The potent compound which has best binding affinity (Score) and one almost a stable interaction with the catalase target was subjected to Molecular dynamics simulations. Molecular dynamics simulations (MD) were run by Nanoscale Molecular Dynamics (NAMD) for 100 ns for the complex (1dgb-compound). The Langevin equation (Toda et al., 1991) is used in NAMD to generate the Boltzmann distribution (canonical NVT, isobar-isotherm NPT) for units and simulations. The Brunger-Brooks-Karplus (BBK) method is used to integrate the Langevin equation (Brünger et al., 1984). The equations of motion (position and velocity) are described by Fokker-Planck (Wang & Skeel, 2003). The detailed analysis of (MD) simulation results of complex-L39 with target catalase is summarized in Figures 7 and 8. Moreover, the stable conformation obtained in the MD simulation of the best complex was conducted by Internal coordinates normal mod analysis server (IMODS). Internal coordinate's normal mode analysis server (IMODS) is a web-based software system. It can be used to investigate the values of deformability, eigenvalues, variance, co-variance map and elastic network. The software package MOE (Molecular Operating Environment) has proven its performance in several recent studies and has been invoked, for example: Stitou et al. (2021), Daoud et al. (2018), Chenafa et al. (2021), Mesli et al. (2019), and Mesli et al. (2021). Among the 60 (according to Table 2) selected compounds the molecular structures of the best compounds were analyzed using a SWISS ADME) server (http://www.swissadme.ch/). The results of absorption, distribution, metabolism and excretion (ADME) for selected compounds are listed in Table 12. These results prescribe that the ADMET-score would be a comprehensive index to estimate chemical drug-likeness. The drug score associate drug likeness, cLogP, LogS, molecular weight and toxicity risks in one handy value than may be attuned to judge the compound's overall potential to quality for a drug (Geronikaki et al., 1999; Lipinski et al., 1997). In this study, prediction and descriptors of druglikeness such as mutagenic, toxicological dosage level were predicted using a PreADMET server (http://preadmet.bmdrc.org/) and admetSAR server (http://lmmd.ecust.edu.cn:8000/). All results of toxicological pathways, including organ toxicity, toxicity and stress response pathways are given in Table 13. To identify the toxicity of the selected best ligands Z-phytol, Eicosane, BHT, EDTA and analogues compounds of L39 and L42, we used Protox II (Banerjee et al., 2018). Cytochromes P450 are key enzymes involved in the metabolism of various endogenous or exogenous molecules. The results of The P450 sites of metabolism (SOM) of the best compound L39 were determined by online tool, RS-WebPredictor 1.0 (Release, 2018) and listed in supplementary Table S11. The

Table 2. Chemical compositions of C. sulphurea essential oils during three developmental stages.

Aerial part of *C. sulphurea* essential oils								
No.[a]	Components	IRI[a,b]	RId[a,c]	RIp[d]	April	May	June	Identification
1	α-Pinene	936	931	1022	3.1	1.7	13.2	RI, MS
2	Sabinene	973	966	1120	–	0.5	5.6	RI, MS
3	β-pinene	978	970	1110	–	0.1	0.9	RI, MS
4	Myrcene	987	981	1159	1.7	0.9	0.2	RI, MS
5	p-Cymene	1015	1011	1265	2.7	0.4	0.3	RI, MS
6	Limonene	1023	1022	1197	4.8	2.7	0.7	RI, MS
7	(Z)-β-ocimene	1024	1026	1230	–	0.1	0.3	RI, MS
8	(E)-β-ocimene	1041	1037	1247	–	0.4	0.2	RI, MS
9	Nonanal	1083	1083	1394	0.7	0.7	0.5	RI, MS
10	Linalool	1081	1088	1544	1.2	tr	tr	RI, MS
11	Terpinen-4-ol	1164	1162	1590	–	0.2	0.1	RI, MS
12	Methyl-Salicylate	1173	1170	1731	–	0.1	0.2	RI, MS
13	Decanol	1185	1185	1498	–	0.2	0.3	RI, MS
14	α-Copaene	1379	1375	1488	–	0.6	3.5	RI, MS
15	(E)-β-Caryophyllene	1424	1418	1591	2.9	1.9	3.4	RI, MS
16	α-Humulene	1456	1450	1665	–	0.4	0.6	RI, MS
17	Germacrene-D	1480	1478	1704	–	0.8	1.1	RI, MS
18	β-Selinene	1483	1482	1712	–	0.6	0.8	RI, MS
19	4-epi-Cubebol	1487	1487	1870	–	0.2	0.6	RI, MS
20	Bicyclogermacrene	1494	1491	1727	–	0.1	0.3	RI, MS
21	α-Muurolene	1496	1493	1719	–	0.1	0.5	RI, MS
22	β-Cadinene	1507	1506	1752	–	0.1	0.2	RI, MS
23	δ-Cadinene	1516	1515	1752	–	0.2	0.5	RI, MS
24	3-(Z)-Hexenyl-benzoate	1554	1550	2088	0.4	0.2	tr	RI, MS
25	Germacrene-D-4-ol	1573	1567	2025	1.3	1.2	0.5	RI, MS
26	Caryophyllene oxide	1576	1571	1980	29.6	27.6	10.5	RI, MS
27	Salvial-4(14)-en-1-one	1584	1580	1996	2.2	2.1	0.2	RI, MS
28	Veridiflorol	1591	1584	2089	12.8	11.5	4.9	RI, MS
29	Humuleneepoxide II	1601	1599	2044	3.9	3.7	6.5	RI, MS
30	ϒ-Eudesmol	1619	1617	2197	2.3	0.9	0.1	RI, MS
31	epi-Cubenol	1624	1623	2059	–	1.9	0.1	RI, MS
32	τ-Muurolol	1634	1630	2103	–	2.1	3.2	RI, MS
33	β-Eudesmol	1644	1640	2232	0.7	7.2	8.5	RI, MS
34	α-Cadinol	1645	1641	2232	0.6	1.1	3.5	RI, MS
35	α-Eudesmol	1653	1649	2220	1.4	2.6	4.5	RI, MS
36	(Z,Z)-Farnesol	1653	1653	2163	0.6	3.1	6.5	RI, MS
37	Eudesma-4(15),7-dien-1β-ol	1672	1670	2347	0.2	3.2	3.2	RI, MS
38	Tetradecanol	1676	1696	2105	–	0.9	0.5	RI, MS
39	(Z)-Phytol	2080	2081	2572	0.1	0.1	0,5	RI, MS
40	Heneicosane	2100	2099	2101	7.3	2.1	0,2	RI, MS
41	(E)-Phytol	2114	2113	2591	5.2	6.3	8,5	RI, MS
42	Eicosane	2200	2201	2200	6.5	1.1	0,2	RI, MS
	Total %				**92.2**	**91.9**	**96.1**	
Oxygenatedmonoterpenes					3.9	1.2	1.1	
Hydrocarbonmonoterpenes					9.6	5.9	20.6	
Hydrocarbonsesquiterpenes					2.9	4.8	10.9	
Oxygenatedsesquiterpenes					55.6	68.4	50.1	
Non-terpeniccompounds					14.9	5.2	4.4	
Oxygenatedditerpenes					5.3	6.4	9.0	
Root parts of*C. sulphurea* essential oils								
43	Hex-3-en-1-ol (E)	812	791	1966	0.4	tr	0.3	RI, MS
44	Hex-3-en-1-ol (Z)	831	825	1380	0.2	tr	0.1	RI, MS
45	α-Thujene	922	923	1023	0.6	1.7	0.3	RI, MS
56	β-pinene	978	970	1110	3.9	2.5	8.1	RI, MS
47	methyl-Salicylate	1173	1170	1731	0.7	0.9	0.5	RI, MS
48	Decanol	1185	1185	1498	2.4	tr	0.8	RI, MS
49	Dec-3-en-2-one	1219	1221	1601	1.3	0.5	0.4	RI, MS
50	Geranylacetate	1361	1367	1752	tr	0.1	0.3	RI, MS
51	α-Copaene	1379	1375	1488	0.1	0.1	0.2	RI, MS
52	Dodecanal	1389	1390	1695	3.4	tr	0.2	RI, MS
53	(E)-β-Caryophyllene	1424	1418	1591	6.5	8.8	16.6	RI, MS
54	α-Humulene	1456	1450	1665	0.5	0.1	tr	RI, MS
55	Germacrene-D	1480	1478	1704	3.5	3.3	1.1	RI, MS
56	Caryophyllene oxide	1576	1571	1980	32.1	19.1	14.6	RI, MS
57	Humuleneepoxide II	1601	1599	2044	1.1	10.6	3.5	RI, MS
58	Aplotaxene	1663	1661	–	27.9	15.5	10.5	RI, MS
59	Hexadecanoicacid	1958	1954		0.2	12.3	5.6	RI, MS
60	(E)-Phytol	2114	2113	2591	10.3	15.4	28.6	RI, MS
Identification %					**95.1**	**90.9**	**91.7**	
Hydrocarbonmonoterpenes					4.5	4.2	8.4	
Oxygenatedmonoterpenes					0.7	0.9	0.5	
Hydrocarbonsesquiterpenes					10.6	12.3	17.9	
Oxygenatedsesquiterpenes					33.2	29.8	18.4	

(*continued*)

Table 2. Continued.

Aerial part of *C. sulphurea* essential oils								
No.[a]	Components	IRI[a,b]	RId[a,c]	RIp[d]	April	May	June	Identification
Oxygenatedditerpenes					10.3	15.4	28.6	
Aliphaticcompounds					35.8	28.3	17.9	

RI: retention indices, MS: mass spectra in electronic impact mode.
[a]Order of elution is given on apolar column (Rtx-1).
[b]Retention indices of literature on the apolar column (IRIA).
[c]Retention indices on the apolar Rtx-1 column (RIA).
[d]Retention indices on the polar Rtx-Wax column.

Table 3. Antioxidant activity (IC_{50}s) of essential oils of *C. sulphurea*.

	Mean values (in g/L) with SD		
Sample name	DPPH radical scavenging (IC_{50})	Metal chelating activity (IC_{50})	β-Carotene/linoleic acid assay (IC_{50})
Aerial part	2.06 ± 0.1	2.02 ± 0.3	38.4 ± 0.5
Root part	1.29 ± 0.5	2.96 ± 0.5	36.6 ± 0.2
BHT (DPPH)	0.26 ± 0.5	–	–
BHT (β-Carotene)	–	–	0.59 ± 0.1
EDTA	–	1.03 ± 0.2	–

SD = standard deviation.

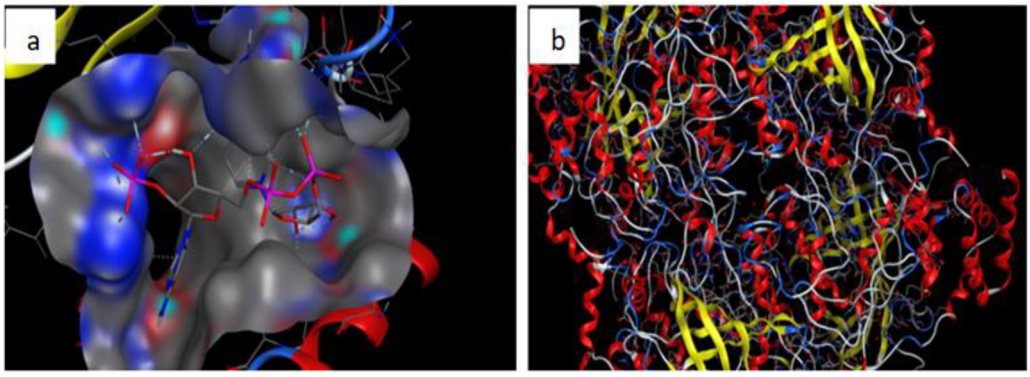

Figure 1. (a) The active site of isolated catalase. (b) Simplified model of catalase.

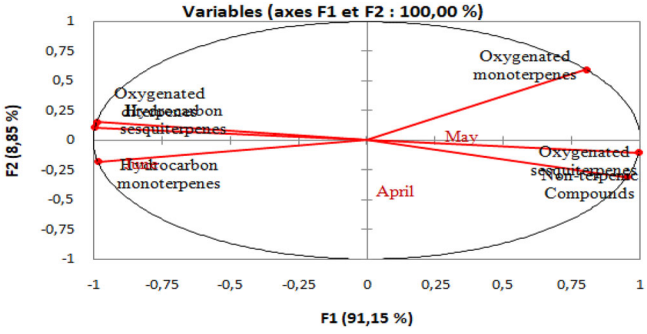

Figure 2. Distribution of variables of chemical composition of Centaurea sulphurea roots during the vegetative cycle.

pharmacophore mapping study of the best ligand was carried out by online server Pharm Mapper (Parr et al., 1989). It consists of identifying common binding elements that is responsible for the biological activity and determining the 3D relationship between pharmacophore elements in each conformation generated (Vyas et al., 2008). The pharmacophore modelling was done for the best ligand molecule among the 60 (according to Table 2) a selected molecule is summarized in Figure 9. However, in this study the P450 sites of metabolism (SOM), toxicological pathways, ligand-based pharmacophore modeling, drug likeness prediction and ADMET-calculations were carried out to determine and compare the biological activities of the two best ligands.

3. Results and discussion

3.1. Experimental approach

3.1.1. Essential oil yields

The essential oil yield of the aerial and root parts of *C. sulphurea* varied remarkably during the three stages of development of the plant. The essential oils yield of aerial and root parts was the lowest (0.05% and 0.15, respectively) during the first vegetative stage. Then it increased appreciably as the floral budding stage outset (0.16% and 0.29%) and reached 0.25% and 0.38% at the flowering stage, respectively (Table 1). This increase in yield can be explained by the length of the vegetative cycle, summer heat and the effect of water stress (Kim et al., 2004; Sangwan et al., 2001).

3.1.2. Chemical composition of C. sulphurea essential oil

The analysis of essential oils of the aerial and root parts of *C. sulphurea* during three stages of development of the plant was analyzed by GC and GC/MS and identified by comparison of their retention indices and mass spectra with those of

Table 4. Energy minimization of the best compounds for antioxidant drug.

Ligand compound		Toxic	LogP	Energies (kcal/mol)	LogS	Hdon + Hacc	Flexibility
L22	β-Cadinene	No	4.58	2.60161e + 001	−4.67	don:0; acc:0	1 out 1
L23	δ-Cadinene	No	4.58	2.95608e + 001	−5.17	don:0; acc:0	1 out 1
L24	3-(Z)-Hexenyl-benzoate	No	3.20	3.01393e + 001	−3.30	don:0; acc:1	6 out 6
L30	Υ-Eudesmol	No	4.06	3.84759e + 001	−3.67	don:1; acc:1	1 out 1
L33	β-Eudesmol	No	3.92	4.47669e + 001	−4.36	don:1; acc:1	1 out 1
L36	(Z,Z)-Farnesol	No	4.40	1.60145e + 001	−4.25	don:1; acc:1	7 out 7
L39	(Z)-Phytol	No	6.36	1.72039e + 001	−8.27	don:1; acc:1	13 out 13
L40	Heneicosane	No	8.44	−8.49952e + 000	−10.66	don:0; acc:0	18 out 18
L42	Eicosane	No	8.05	−8.29676e + 000	−10.15	don:0; acc:0	17 out 17
L50	Geranyl acetate	No	3.24	9.02954e + 000	−3.02	don:0; acc:1	6 out 6
L58	Aplotaxene	No	5.98	1.22114e + 001	−7.27	don:0; acc:0	11 out 11
L59	Hexadecanoic acid	No	5.55	−1.46061e + 001	−6.49	don:2; acc:1	14 out 14
L60	(E)-Phytol	No	8.27	1.77210e + 001	6.36	don:1; acc:1	13 out 13

Table 5. S-score (Energy) and interactions between best compounds and the active site residues of catalase target.

			Bonds between atoms of compounds and residues of the active site					
No.	Compounds	S-score (kcal/mol)	Atom of compound	Involved receptor atoms	Involved receptor residues	Type of interaction bond	Distances (Å)	Energy (kcal/mol)
	Catalase (Cal)							
L59	Hexadecanoic acid	−6.266	6-ring	OH	TYR 215	H-acceptor	2.26	63.6
				O	HOH 1533	H-acceptor	3.51	−0.6
L60	(E)-Phytol	−6.882	O1 1	O	HOH 1558	H-acceptor	2.88	−0.3
			O1 1					
L39	(Z)-Phytol	−7.184	O1	NZ	LYS237	H-acceptor	3.11	−1.80
L40	Heneicosane	−6.900	C 12	5-ring	HIS 305	H-pi	3.62	−0.7
L42	Eicosane	−7.158	C-11	6-ring	PHE198	H-Pi	4.45	−0.60

H = Conventional hydrogen bond, C = Carbon hydrogen bond, Aa = Alkyl-alkyl, Ap = Alkyl-Pi, Aps = Amide-Pi stacked, Ppt = Pi-pi T-shaped, X = Halogen.

the "Aromas" library specific to the laboratory of the University of Corsica. The chemical compositions are presented in Tables 2 and 3. Eight monoterpene hydrocarbons, nine sesquiterpene hydrocarbons, three oxygenated monoterpenes, sixteen oxygenated sesquiterpenes, four oxygenated diterpenes and two non-terpenic compounds were identified in the aerial parts. Throughout the vegetative cycle (May–June), the essential oil of aerial parts has been characterized by a high percentage of oxygenated sesquiterpenes characterized by caryophyllene oxide (10.5–29.6%), verridiflorol (4.9–12.8%) and humulene epoxide II (3.7–6.5%). At the vegetative stage and the floral budding stage, the hydrocarbon monoterpenes and the hydrocarbon sesquiterpenes were present in low amounts with percentages varying from 1.2–3.9% and 5.9–9.6%. Then at the flowering stage, they increased at 20.6% and 10.9%, respectively (Table 2). At the vegetative stage (May), the aliphatic compounds were more predominant (14.9%) followed by heneicosane (7.3%) and eicosane (6.5%) (Table 2).

The chemical compositions of root parts are presented in Table 3. Eighteen components were detected, accounting for 95.1% at the vegetative stage, 90.9% at the floral budding and 91.7% at the flowering stage. The essential oil of root parts of vegetative stage contains aliphatic compounds (35.8%), oxygenated sesquiterpenes (33.2%), hydrocarbon sesquiterpenes (10.6%) and oxygenated diterpenes (10.3%) (Table 2, Figure 1). The oil contains caryophyllene oxide (32.1%), aplotaxene (27.9%) and (E)-phytol (10.3%) as main components. At the floral budding, the essential oil of *C. sulphurea* was dominated by oxygenated sesquiterpenes (29.8%) and aliphatic compounds (28.3%), followed by oxygenated diterpenes (15.4%) and hydrocarbon sesquiterpenes (12.3%) (Figure 1). The main components were caryophyllene oxide (19.1%), aplotaxene (15.5%), (E)-phytol (15.4%) and hexadecanoic acid (12.3%). On the other hand, at the flowering stage, the oil of roots was dominated by oxygenated diterpenes (28.6%), oxygenated sesquiterpenes (18.4%), aliphatic compounds (17.9%), hydrocarbon sesquiterpenes (17.9%) and small amount of hydrocarbon monoterpenes (8.4%) (Table 2 and Figure 2). The main components were (E)-phytol (28.6%), (E)-β-caryophyllene (16.6%), caryophyllene oxide (14.6%), aplotaxene (10.5%) and β-pinene (8.1%). It is noteworthy that the normalized percent abundances of major oil components varied greatly according to physiological stage.

A significant increase in hydrocarbons sesquiterpenes were observed with a percentage for 10% at the vegetative stage to 18% at the floral stage compared to oxygenate which decreased (33% to 18%). However, caryophyllene oxide and aplotaxene, showed a significant decrease of their percentage during vegetative monitoring (32 to 14%) and (27 to 10%), respectively. However, the content of oxygenated diterpenes increased significantly at the budding and flowering stages, with a percentage of 15.4% and 28.6% respectively. While the content of aliphatic compounds was at 35.8% decreased to 17.9% at the flowering stage (Table 2).

From our results cited in Table 2, we were able to trace the variation in the contents of the different chemical classes of essential oils from roots *C. sulphurea* see Figure 2. The distribution (Figure 2) showed that the essential oil was rich in oxygenated sesquiterpenes (18.4–33.2%) and aliphatic components (17.9–35.8%) during the month of April. However, the percentage of hydrocarbon sesquiterpenes was relatively

Table 6. The docking energies of **best** DNA inhibitors.

Ligand	Compound	**DE*** **(kcal/mol)** *ctDNA*	DE* (kcal/mol) *Catalase*	ETOR (kT)	VDW (kT)	EIE (kT)
BHT31404		−4.743	−5.052	330.721	413.487	−1942.09
EDTA6049		−4.965	−5.591	330.722	413.486	−1942.09
Lref		−5.900	−8.043	330.722	413.486	−1942.09
L39	(Z)-Phytol	−6.978	−7.184	330.723	413.317	−1942.01
L40	Heneicosane	−6.819	−6.809	330.724	413.316	−1942.01
L42	Eicosane	−6.858	−7.158	330.724	413.316	−1942.01
L59	Hexadecanoic acid	−6.516	−6.266	330.725	413.315	−1942.01
L60	(E)-Phytol	−6.425	−6.908	330.720	413.488	−1942.09

DE: Energy, ETOR: Energy Torsion, VDW: Van Der Walls, EIE: Electrostatic.

Table 7. Interaction profiles of the **potential** compounds for three *Endogenous Enzymatic* inhibitors.

No.	Compound	Targets	Energy (kcal/mol)	Energy torsion (kT)	Van Der Walls (kcal/mol)	Electrostatic (kcal/mol)
Lref	NADPH	CAT	−8.043	2603.149	8687.066	−22,383.8
		SOD	−3.247	637.836	3687.273	−10,233.1
		GPX	−6.176	1134.834	4767.672	−12,474.1
L39	(Z)-Phytol	CAT	−7.184	2537.734	8664.659	−22,264.6
		SOD	−3.993	598.608	4192.510	−10,291.6
		GPX	−4.413	1091.834	4753.317	−12,384.3
L40	Heneicosane	CAT	−6.809	2522.562	8677.642	−22,285.8
		SOD	−4.142	581.009	3691.151	−10,289.5
		GPX	−4.340	1054.875	4788.068	−12,421.7
L42	Eicosane	CAT	−7.158	2515.807	8661.011	−22,263.4
		SOD	−4.163	581.203	3704.941	−10,281.9
		GPX	−4.686	1060.625	4773.694	−12,419.8
L59	Hexadecanoic acid	CAT	−6.266	2527.458	8649.425	−22,338.3
		SOD	−3.617	590.860	3763.376	−10,415.7
		GPX	−4.748	1077.965	4792.381	−12,482.6
L60	(E)-Phytol	CAT	−6.882	2533.186	8651.835	−22,244.0
		SOD	−3.798	598.256	3744.463	−10,344.5
		GPX	−5.281	1067.257	4775.731	−12,435.8

DE: docking energy; ETOR: Torsion energy; VDW: Van der Waals; EIE: Electrostatic Interaction Energy.

lower (4.2–8.4%) compared to oxygenated sesquiterpenes during the month of June. The, oxygenated monoterpenes (0.–-.09%) constitute the lowest percentage classes during the month of May. Previous work has shown that the main components of essential oils of *C. dimorphaViv.* and *C. apiculata Lebed* collected in Algeria and Bulgaria, respectively were rich in caryophyllene oxide with a percentage of (9.9% and 15.8%) (Belkassam et al., 2019; Riccobono et al., 2017). However, hexadecanoic acid was detected as main constituent in essential oils of *C. pterocaula Trautv* (Sen et al., 2021), *C. aggregata subsp. aggregata, C. balsamita* and *C. Behen* (Erdogan et al., 2017) from Turkey with a percentage ranging from 23.0% to 35.8%, similarly for essential oil from Lebanon (33.2%) (Senatore et al., 2005). On the other hand, the main component obtained from the essential oils of *C. pumilio* from Egypt was pentadecane (17.8%) (Naeim et al., 2020), *C. damascena* from Jordan was fokienol (11.4%) (Khleifat et al., 2019), *C. polymorpha* from Spain was Heptacosane (11.5%) (Formisano et al., 2006) and *C. grinensis* from Croatia was p-vinyl guaiacol (21.5%) (Riccobono et al., 2017). Benzyl benzoate (26.5%) and geranial (38.6%) were detected as the main constituents of essential oils of *C. ispahanica Boiss* and *C. irritans* from Iran, respectively (Formisano et al., 2006; Khleifat et al., 2019). The essential oils of *C. grisebachii* subsp. *Grisebachii* and *C. affinis* Friv. from Greece were dominated by 6,10,14-trimethyl-pentadecan-2-one (12.9%) and tetracosane (7.8%) (Djeddi et al., 2011). Essential oils of *C. paniculata* Subsp. *Carueliana* and *C. rupestris* from Italy were constituted by (Z)-3-hexenol (16.5%) and germacrene D (42.3%) (Tava et al., 2010).

3.1.3. Evaluation of the antioxidant activities of essential oils

The antioxidant activities were performed using the free radical scavenging activity (DPPH), metal chelating tests and β-carotene bleaching assay, using BHT and EDTA as a positive control (Table 3).

The free radical scavenging activity of *C. sulphurea* essential oil was analyzed using DPPH assay. Varying concentrations of the samples were used from 0.2 to 15 g/L. It has been observed that the free radical scavenging activity increases with the increase in concentration oils (Table 3). It is also observed that the aerial and root parts of essential oils had good antioxidant activity, with IC_{50} values of 2.06 g/L and 1.29 g/L, respectively, but this activity remains lower compared to the BHT control (IC_{50} =0.26 g/L).

Chelating activity on Fe^{+2} of essential oils of *C. sulphurea* was estimated using various amounts of oil from 0.2 to 15 mg/mL. From the IC_{50} values obtained, it was observed that the oil of the aerial part (IC_{50} = 2.02 g/L) exhibited a greater inhibitory activity than the essential oil of the root part (IC_{50} = 2.96 g/L), while that of the EDTA control, the IC_{50} was 1.03 g/L (Table 3). These oils either chelated metal ions or suppressed reactivity by occupying all coordination sites of metal ions (Mohaney et al., 1985).

β-carotene-linoleic acid activity of essential oils of *C. sulphurea* was estimated using various concentrations from 5.0 to 38 g/L for essential oils and 0.1 to 8.0 g/L for BHT. From the IC_{50} values obtained, it has been observed that the oil from the root part showed a greater inhibitory activity with an IC_{50} of 36.6 g/L contrary to the aerial part (IC_{50} = 38.4 g/

L). The standard has the highest activity with an IC_{50} of 0.59 g/L. The rate of β-carotene bleaching can be slowed down in the presence of antioxidants (Oke et al., 2009). Indeed, this last one is a free radical mediated phenomenon resulting from the hydroperoxides formed from linoleic acid, which attack the highly unsaturated β-carotene molecules (Wang et al., 2008).

It can be concluded that the essential oils of *C. sulphurea* showed significant antioxidant potential, presumably due to qualitative and quantitative difference of their components. This antioxidant effectiveness of aerial and root parts essential oils may be attributed primarily to the presence of (E)-β-caryophyllene and caryophyllene oxide in high concentrations. Indeed, it has been previously shown that species rich in these compounds possessed appreciable antioxidant activity (Figueiredo et al., 2019; Sarikurkcu et al., 2018; Nafis et al., 2019). Also, the activity of the root part could be explained by the presence of the dominating compound aplotaxene, but to our knowledge there are no studies on evaluation of the antioxidant capacity of hydrocarbons compounds.

3.2. Theoretical and computational methods

3.2.1. Evaluation of molecular docking

3.2.1.1. Properties of compounds. The information of best compounds after docking was obtained from MOE software (Molecular Operating Environment (MOE), 2019) and Molegro Virtual Docker (MVD) software (Thomsen et al., 2006) given for ligands in Table 4 and properties of other compounds of aerial and root part of *C. sulphurea* are listed in Tables S1 and S2 (Supplementary Materials), respectively.

According to the table above, we note also that the five molecules (Z)-phytol, heneicosane, eicosane, hexadecanoic acid and (E)-phytol have a high value of flexibility compared to other molecules and also the results obtained show that these five ligands have a high value of torsion angle relative to other compounds. This shows that these compounds L39, L60, L59, L40 and L42 are more flexible. In addition, it is noted that the growth of the torsion angle depends on the binding number of the compound.

3.2.1.2. Identification of the best poses based on affinity of compounds with catalase target. The results obtained after the docking calculations and the **five best poses** received for the best compounds with the pocket of the ***catalase*** target have been listed in Table 5 and the results of energy (binding affinity) for other compounds are listed in Tables S3–S5 (Supplementary Materials).

3.2.1.3. Interaction with catalase, CtDNA sequence and endogenous enzymatic antioxidant systems

3.2.1.3.1. Interaction with catalase. The results obtained show that the scores of binding free energies of all complexes (1dgb-compound) were between −3.819 and −7.184 kcal/mol and the complexes formed by compounds: L39 and L42 have the lowest score of binding energy compared to the other complexes (see Table 5; Tables S3–S5, Supplementary Materials). They give the best docking scores, based on the binding free energy (Table 5). This shows that these complexes are more stable. As can be seen from Figure 3 and Figure 4.

Table 8. Thermodynamic properties calculated in reels units.

Stage	Method	H	U	EKT	P	V
SP_1	CATNVT	−548.001	1239.506	7896.099	−60.342	70,733.242
	CATNPT	126.562	−3738.745	3258.956	−166.790	70,734.429
	CATNVT	−3.077	−1794.187	6340.632	−6.647	70,733.242
	CATNPT	0.607	−4177.466	3644.816	−25.583	70,129.531
	CATNVT	1.431	−1872.646	296.267	47.574	70,733.242
	CATNPT	0.856	−4300.242	3777.552	−44.703	68,616.622
SP_2	CATNVT	1.794	−1910.387	6454.985	110.509	70,733.242
	CATNPT	1.732	−4370.358	3851.464	−19.527	68,023.101
	CATNVT	7.922	−2034.435	6380.051	−48.245	70,733.242
	CATNPT	15.996	−4431.202	3926.552	−21.916	66,554.343
	CATNVT	6.380	−2223.329	6466.652	−91.712	70,733.242
	CATNPT	24.248	−4429.957	3933.550	−81.352	65,744.632
SP_3	CATNVT	−1.253	−2267.157	6466.531	50.258	70,733.242
	CATNPT	4.536	−4482.546	4055.145	108.319	58,992.375
	CATNVT	0.874	−2352.489	6388.428	−44.417	70,733.242
	CATNPT	44.459	−4455.767	4068.258	−34.409	55,208.097
	CATNVT	5.273	−2387.140	6402.313	61.308	70,733.242
	CATNPT	87.701	−4490.880	4146.594	153.381	51,238.800

Pressure $P = P^* \varepsilon / \sigma^{-3}$. Energy of configuration $U = U^* N\varepsilon$. Translation Kinetic Energy $EKT = EKT^* N\varepsilon$ and Enthalpy $H = H^* N\varepsilon$.

We note that the complex formed by the compound L39 (1dgb-L39) has the lowest energy score compared to the other complexes formed by control test butyled hydroxyltoluene (BHT) and ethylenediaminetetraacetic acid (EDTA). Moreover, this compound forms one interaction with active site residue of the catalase target.

The complex formed by compound L42 gave a score value very close (slightly higher) to the value of the both best of control test butyled hydroxyltoluene (BHT) and ethylenediaminetetraacetic (EDTA) (Table 5). Their binding free energies were −5.052 and −5.591 kcal/mol respectively. In addition, this compound establishes one interaction with active site residues of the catalase target.

In addition, other compounds that formed interactions with active site residues of the catalase target which are less stable than L39 and L42 are given in Tables S3–S5 (Supplementary Materials). These ligands are 3-(Z)-hexenylbenzoate, β-eudesmol and (E)-phytolligands L24, L33, L60, interacts with LYS 237 (pi-cation), PHE 198 and HOH 1558 at a distance of 3.83, 4.49 and 2.08 Å strong with energy of −1.3, −0.7 and −0.3 kcal/mol respectively and p-cymene ligand L5 interacts with one amino acid PHE 198 pi-pi at a distance of 3.89 Å strong and energy binding of −0.04, similarly, the α-copaene, β-cadinene, salvial-4(14)-en-1-one ligand (L14, L22 and L27) interacts with H-pi at a distance of 3.77, 4.00 and 3.80 Å (strong, low) respectively. Humuleneepoxyde II, τ-muurolol and β-eudesmol ligands (L29, L32 and L33) interacts with HIS 305, H-pi, HOH 1444 and HOH 1533 at a distance of 3.75, 2060 and 2.72 Å (weak) respectively with energy binding of −1.0; −1.1 and −1.2 kcal/mol respectively while (Z,Z)-farnesol ligand (L36) interacts with HOH 1465 H-donor at a distance of 2.59 Å (strong) and energy binding of −0.6 kcal/mol. Hexadecanoic acid, linalool, methyl-salicylate and decanol interacts with one amino acid TYR 215, ARG203 and HOH 1414, HOH 1484 H-acceptor at a distance of 2.26, 2.63, 4.33 and 2.64, 2.34 Å average, strong interaction and energy binding of −6.6, −1.5, −0.7 and −0.4 kcal/mol, and

Table 9. Predicted toxicity risks of **best** test compounds.

Ligands	Mutagenic	Tumorigenic	Irritant	Reproductive effective
Lref				
BHT				
EDTA				
L39				
L40				
L42				
L59				
L60				
1-Analog structure L39				
2-Analog structure L39				
3-Analog structure L39				
4-Analog structure L39				

Green = good, yellow = tolerable, red = bad.

interaction with heneicosane, α-thujene, methyl-salicylate, decanolanddec-3-en-2-one with HIS 305, PHE198, ASN 149 and HOH 1465, respectively, H-donor and H-pi at a distance of 3.62,4.21, 2.47 and 2.54 Å (strong, low, average interaction) and energy binding of −0.7, −0.6.0.4 and −0.8 kcal/mol respectively. Dec-3-en-2-one, geranylacetate, dodecanal and caryophyllene oxide interact with HOH 1465–1533, HIS305, HOH1068 and HIS305 with energy binding of −1.7, −3.6, −2.7 and −0.6 kcal/mol.

In our research, all the compounds tested show stable hydrogen bonds. On the other hand, previous research (Sarwar et al., 2010, 2013) proved that, halogen bonding similar to hydrogen bonding plays a crucial role for biological and chemical systems.

The binding affinity of L39, L42, L40, L60, and L59 ((Z)-phytol, eicosane, heneicosane, (E)-phytol and hexadecanoic acid) have considerably increased to −7.184,−7.158, −6.900, −6.882, and −6.266 kcal/mol respectively. Improved hydrogen bond was observed in L39 and L42. This bond not only contribute in increasing binding affinity, but also enhance the binding specificity (Bissantz et al., 2010; Sarwar et al., 2013). This observation helped to confirm that compounds (L39 and L42) (oxygenated diterpene) are bound at the desired binding site of receptor protein after molecular docking.

3.2.1.3.2. Interaction mechanism of the complex with Ct-DNA sequence. According to the research of (Birben et al., 2012) reactive oxygen species (ROS) can lead to DNA modifications in several ways, which involves degradation of bases, single- or double-stranded DNA breaks, purine, pyrimidine, or sugar. Most of these DNA modifications are highly relevant to carcinogenesis, aging, and neurodegenerative, cardiovascular, and autoimmune diseases (Al-Dalaen et al., 2014). So, this study was to elucidate the interaction of the best ligands obtained by molecular docking with the *CtDNA* sequence, in order to validate the interactions with the nucleotides and their affinities. The results obtained after the docking calculations for the **five** best compounds with the pocket of the *Ct-DNA* sequence (CGCGAATTCGCG)2 dodecamer (PDBID:1BNA) have been listed in Table 6. Energy (binding affinity) and interactions for other compounds are listed in Table S6 (Supplementary Materials).

The obtained results show that compounds with stronger electron—donating substituents have higher DNA-binding ability than the others; On the other hand, results show that some of the tested compounds are minor groove binders. Our results demonstrated that the five compounds: (Z)-phytol (Ligand 39), eicosane (Ligand 42), heneicosane (Ligand 40), hexadecanoic acid (Ligand 59), aplotaxene (Ligand 58), and (E)-phytol (Ligand 60), were the best interacting compounds (see Table 6; Supplementary Materials Table S6).

The calculated docking energies for these compounds were respectively −6.978, −6.858, −6.819, −6.516, −6.425, and −6.4.6 kcal mol^{-1}. With the exception of β-cadinene, ϒ-eudesmoland β-eudesmol, other compounds are located in the small cDNA groove. The results of molecular docking showed that β-cadinene, ϒ-eudesmol and β-eudesmol, existed in the main groove region. The calculated docking energy of this compound was −4.741, −4.824 and −4.793 kcal mol^{-1}, respectively (See Supplementary Materials Table S6). Among, the test candidates in this study, (Z)-phytol (Ligand 39), eicosane (Ligand 42), displayed the lowest binding energy of −6.978, −6.858 kcal/mol for Ct-DNA sequence and −7.184, −7.158 kcal/mol for the enzyme. These energies are lower compared to those of the Lref (NADPH) and two control ligands butylated hydroxyltoluene (BHT) and ethylenediaminetetraacetic acid (EDTA). Their binding energies obtained are −4.743, −4.965 kcal/mol, respectively for DNA sequence and −5.052, −5.591 kcal/mol, respectively, for the enzyme were much higher than (Z)-phytol, as found in our study; thus (Z)-phytol (Ligand 39), eicosane (Ligand 42) displayed much better binding than the Lref (NADPH) and control molecule; butylated hydroxyltoluene (BHT) and ethylenediaminetetraacetic acid (EDTA). The two complexes are showing greater antioxidant activity than butyled hydroxytoluene (BHT) and ethylene diaminetetraacitic acid (EDTA).

The docking results reveal that the binding strength of complex-1 [(Z)-phytol-catalase] is higher than complex-2 [eicosane-catalase]. Molecular dynamics simulation studies suggest that compound (Z)-phytol has a strong *DNA*-binding affinity than compound eicosane. The more bonding strength of complex-1 is due to the presence of hydrophobic pi-pi interactions with nucleotide bases of *DNA*, along with hydrogen bonding interaction. On the other hand, complex-2 eicosane-catalase showed only a few pi-pi interactions with nucleotide bases of *DNA*. The bulkier aromatic group in complex-1 participated in pi-pi interactions with nucleotides. However, the group in eicosane-catalase showed no interactions with nucleotides. Thus, the absence of pi-pi interactions with DC15 and DT14 nucleotides lowers the binding affinity of complex-2.

From the docking results with the optimal energy, it was found that the complex [complex-1 (Z)-phytol-catalase] inserted into the groove of *DNA* fragments and hydrophobic forces play main roles in the binding of complex to ct-*DNA*.

The docking results reveal (Z)-phytol and eicosane displayed much better binding (See Figure 5). From our results, we can conclude that complex-1 showed greater *DNA* binding and antioxidant activity than complex-2.

3.2.1.3.3. Interaction with endogenous enzymes antioxidant systems. In order to complete this research, we deemed it

Table 10. In silico Bioisosteric Replacement based on similarity comparison method using MolOpt.

Molecule	Replaceable group	Transformation in previous studies	Analogue structure	Smiles
L39 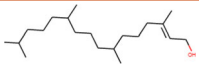	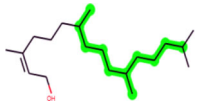	Eur. J. Biochem., 1989, 185, 605–614	1-Analog L39 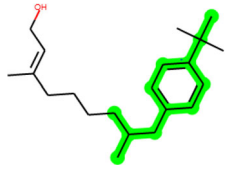	CC(=CCO)CCCCC (C)Cc1ccc(C(C)(C)C)cc1
	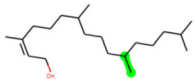	Drug Metab. Dispos., 2012, 40, 928–942 J. Med. Chem., 2008, 51, 3720–3730	2-Analog L39 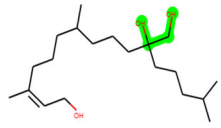	CC(=CCO)CCCC(C) CCCC(O)(CO)CCCC(C)C
	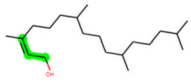	J. Nat. Prod., 2004, 67, 1783–1788	3-Analog L39 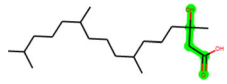	CC(C)CCCC(C)CCCC(C) CCCC(C)(O)CC(=O)O
	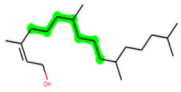	J. Nat. Prod., 2004, 67, 1783–1788	4-Analog L39 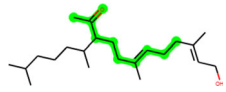	CC(=O)C(CCC(C) =CCCC(C)=CCO)C(C)CCCC(C)C

useful to study the interaction of our best molecules with other defense systems antioxidant targets such as SOD and GPX.

The results of docking energies of three endogenous enzymes and five best inhibitors are shown in (Table 7). And results of other compounds are shown in Table S7 (Supplementary Materials).

Molecular docking results revealed that (Z)-phytol (Ligand 39), eicosane (Ligand 42), (E)-phytol (Ligand 60), heneicosane (Ligand 40), hexadecanoic acid (Ligand 59), and aplotaxene (Ligand 58) were the best compounds interacting with the suspected binding residues at the active site catalase (Figure 6; Supplementary Materials). The calculated docking energies for these molecules were respectively −7.184, −7.158, −6.882, −6.809, −6.266, and −6.130 kcal mol^{-1}. β-eudesmol and Υ-eudesmol were the weakest interacting compounds with this receptor (Table S7 Supplementary Materials). The calculated docking energy, calculated for this compound was −5.070 and −5.286 kcal mol^{-1}, respectively. The best compounds, interacting with the suspected binding residues at the active site superoxide dismutases*is* (Z)-phytol (Ligand 39), eicosane (Ligand 42), (E)-geranyl acetate (Ligand 50), heneicosane (Ligand 40) (Table 7; Supplementary Materials Table S7). The calculated docking energies for these molecules were respectively −3.993, −4.163 and − 4.173, −4.142 kcal mol^{-1}. β-cadinene and Υ-eudesmol (Table S7, Supplementary Materials) was the weakest interacting compound with this receptor. The calculated docking energy calculated for this compound is −3.422 and −3.182 kcal mol^{-1}, respectively. Additionally, the best compounds interacting with the suspected binding residues at the active site glutathione peroxidase were (E)-phytol (Ligand 60), hexadecanoic acid (Ligand 59), eicosane (Ligand 42), aplotaxene (Ligand 58) (Supplementary Materials Table S7). The calculated docking energies for these molecules were respectively −5.281, −4.748, −4.686, and −4.664 kcal mol^{-1}. β-eudesmol and δ-cadinene were the weakest interacting compound with the receptor glutathione peroxidase. The calculated docking energy calculated for this compound are −4.000 and −4.053 kcal mol^{-1}, respectively. We observed that (Z)-phytol (Ligand 39), eicosane (Ligand 42), heneicosane (Ligand 40), hexadecanoic acid (Ligand 59), aplotaxene (Ligand 58), and (E)-phytol (Ligand 60) showed a binding affinity for interacting with receptors for ctDNA and the same compounds showed a binding affinity for catalse and site of glutathione peroxidase but these compounds (Z)-phytol (Ligand 39), eicosane (Ligand 42), (E)-geranyl acetate (Ligand 50), heneicosane (Ligand 40) showed a binding affinity for interacting with receptors for superoxide dismutase. Representations of the best pose interactions (Z)-phytol (Ligand 39), eicosane (Ligand 42), with three targets (CAT, SOD and GPX) are shown in Figure S1 (Supplementary Materials).

3.2.2. Evaluation of molecular dynamics

Many previous studies (Chen et al., 2014, 2015; Hung et al., 2014) confirmed that the highest dock score obtained by molecular docking does not mean that the compound is a potent lead. Therefore, to validate this result it is necessary to carry out molecular dynamics simulations. From the docking results, Z-phytol was found to possess the best binding affinity towards the Endogenous enzyme. Hence, the complex of Z-phytol with catalase was subjected to 100 ns of MD simulation.

3.2.2.1. Thermodynamic properties. We have studied the evolution thermodynamic properties of best ligand (Z)-phytol (Ligand39) in the NVT and NPT ensemble. We performed energy minimizations of the best complex after docking of 600 ps. Then carried out simulations up to (MD production cycles) 100 ns in three stages under constraints (see Table 8).

An important point is also obtained from Table 8. The translation and rotation energies of the complex formed by the ligand L39 in NPT are very important. Unlike the complex formed by the same ligand in NVT ensemble, these energies and its enthalpy are low. Pressure fluctuations in NVT units are greater than NPT units. Therefore, (Z)-phytol (Ligand 39) is predicted

Table 11. Drug-likeness prediction and Physicochemical Properties (PC) through OSIRIS property explorer and the Swiss ADME online server of the **best** inhibitors.

		Drug likeliness						Physicochemical properties (PC)			
S. no.	Ligand	*c* log *P*	Solubility log *S*	Molecular weight	TPSA Å^2	Drug likeness	Drug score	Refra.	Lipophi.	**Solub.**	Skin perm.
BHT		4.82	−3.98	220.35	20.23	−9.12	0.05	71.97	3.33	−5.27	−4.02
EDTA		−6.14	1.67	292.24	155.6	−7.63	0.17	63.06	−0.05	2.78	−12.26
Lref		−11.59	0.95	745.2	393.5	−36.39	0.26	156.1	−0.21	0.57	−15.70
01	L39	7.42	−4.63	296.54	20.23	−3.77	0.27	98.94	4.78	−5.98	−2.29
02	L40	9.61	−6.11	296.56	00.00	−20.40	0.24	103.0	5.58	−7.41	−0.31
03	L42	9.16	−5.84	282.55	00.00	−20.40	0.24	98.25	5.64	−7.05	−0.60
04	L59	6.06	−4.24	256.43	37.30	−25.22	0.11	80.80	3.85	−5.02	−2.77
05	L60	7.42	−4.63	296.54	20.23	−3.77	0.27	98.94	4.77	−5.98	−2.29
1-Analog	L39	6.83	−4.72	302.50	20.23	−8.02	0.17	99.44	4.48	−5.72	−3.19
2-Analog	L39	5.63	−3.68	328.53	60.69	−5.99	0.32	101.3	4.29	−4.21	−4.63
3-Analog	L39	6.08	−4.43	328.53	57.53	−2.67	0.32	101.2	4.27	−7.72	−3.54
4-Analog	L39	7.18	−4.45	336.56	37.30	−3.09	0.16	108.2	4.58	−5.22	−3.67

MW: molecular weight, MLogP: logarithm of partition coefficient of the compound between water and n-octanol: log: solubility; TPSA or Topological Polar Surface Area: the surface belonging to polar atoms in the compound.
Refra: Molar Refractivity, Lipophi: Lipophilicity , Solub: Water solubility, Skin perm: skin permeation.

Table 12. Pharmacokinetic and toxicity evaluated parameters of best compounds.

		39	1-Analog structure **L39**	2-Analog structure L39	3-Analog structure **L39**	4-Analog structure L39	42
Absorption	Human intestinal	90.643	92.051	90.594	90.706	93.967	89.671
	Skin permeability	−2.631	−2.564	−2.663	−2.735	−2.586	−2.774
	Caco-2 permeability	1.399	1.44	1.666	−2.735	1.497	1.371
	Water solubility[a]	−5.51 MS	−6.36 PS	−4.37 MS	−4.83 MS	−5.11 MS	−7.94 PS
Distribution	VDss (human)	0.385	0.703	−0.377	−0.782	0.036	0.614
	BBB permeability	0.793	0.729	−0.374	−0.225	−0.299	1.014
	CNS permeability	−1.527	−0.728	−2.767	−2.604	−1.796	−1.199
Excretion	Total clearance	1.686	1.444	1.759	1.49	1.854	1.998
	Renal organic cation transporter	No	No	No	No	No	No
Toxicity	Oral rat acute toxicity (LD50)	1.848	2.566	3.272	1.653	1.973	1.586
	AMES toxicity	No	No	No	No	No	No
	Minnow toxicity	−1.137	−0.543	0.178	−1.121	−1.025	−2.372

Green = good, yellow = tolerable , red = bad.
MS: Moderately soluble, PS: Poorly soluble.
Active components: 39—(Z)-Phytol, 42—Eicosane. BBB: Blood-brain barrier.
ADMET: Absorption, distribution, metabolism, excretion and toxicity.
VD_{SS}: < -0.15 low, >0.45 high, BBB: >0.3 cross BBB, < -1 poorly distributed to the BBB, CNS: > -2 penetrate CNS, < -3 unable to penetrate CNS, Low skin permeability: > -2.5, Caco-2 permeability: > 0.9, Human intestinal absorption: > 90.
[a]Results from SwissADME tools.

Table 13. Organ Toxicity, toxicity and Stress response pathways report of the best two molecules analogues and two ligands of control.

Ligands			L 39	Analog 01	Analog 02	Analog 03	Analog 04	L 42	(BHT)	(EDTA)
Predicted LD50 mg/kg			5000	6750	5000	4820	5000	750	650	5000
Predicted Toxicity Class			5	6	5	5	5	3	4	2
	Target			**Prediction / Probability**						
Classification	Organ toxicity	Hepatotoxicity	I 0.79	I 0.79	I 0.85	I 0.68	I 0.73	I 0.74	I	I
	Toxicity	Carcinogenicity	I 0.76	I 0.76	I 0.61	I 0.67	I 0.77	I 0.58	I	A
		Immunotoxicity	I 0.99	I 0.98	I 0.98	I 0.99	I 0.99	I 0.98	I	I
		Mutagenicity	I 0.97	I 0.71	I 0.75	I 0.85	I 0.94	I 1.0	I	I
		Cytotoxicity	I 0.85	I 0.82	I 0.86	I 0.85	I 0.87	I 0.78	I	I
	Stress response pathways	Nuclear factor (erythroid-derived 2)-like 2/antioxidant responsive element (nrf2/ARE)	I 0.98	I 0.71	I 0.92	I 0.97	I 0.96	I 1.0	I	I
		Heat shock factor response element (HSE)	I 0.98	I 0.71	I 0.92	I 0.97	I 0.96	I 1.0	I	I
		Mitochondrial Membrane Potential (MMP)	I 0.99	I 0.58	I 0.85	I 0.97	I 0.98	I 1.0	A	I
		Phosphoprotein (Tumor Supressor) p53	I 1.0	I 0.99	I 0.98	I 0.98	I 0.99	I 1.0	I	I
		ATPase family AAA domain-containing protein 5 (ATAD5)	I 1.0	I 0.99	I 0.98	I 0.98	I 0.99	I 1.0	I	I

A: Active, **I:** Inactive.

to be the most interactive system. These results are in total agreement with the docking prediction results (see Tables 7 and 8). Thermodynamic parameters in agreement with molecular docking results demonstrated that schiff base complexes could combine with catalase spontaneously through hydrogen bonds and Van der Waals interactions.

Table 14. Energy balance of complexes formed with Catalase (*Cat*) under potent clinical antioxidant, some species of *Centaurea* and our results for essential oils of the *Sulphurea*.

Some species of Centaurea.				
Other experiments				
Country	Score	Species	Major components	Reference
Algeria	−4.745	*C. dimorpha Viv.*	caryophyllene oxide (9.88%)	(Belkassam et al., 2019).
Turkey (Patnos)	−6.222	*C. pterocaula Trautv*	Hexadecanoic acid (13.9%)	(Sen et al., 2021).
Turkey (Elazığ)		*C. aggregata subsp. Aggregata*	Hexadecanoic acid (35.8%)	(Erdogan et al., 2017).
		C. balsamita	Hexadecanoic acid (23.0%)	
		C. behen	Hexadecanoic acid (32.7%)	
Egypt	−5.635	*C. pumilio L*	Pentadecane (17.8%)	(Naeim et al., 2020)
Iran (Sofeh-Isfahan)	−5.282	*C. ispahanica Boiss*	Benzyl benzoate (26.5%)	(Firouznia et al., 2007). (Ayromlou et al., 2020)
Iran (Mehran)	−4.809	*C. irritans*	Geranial (38.6%)	
Italy	−4.517	*C. paniculata Subsp. Carueliana*	(Z)-3-hexenol (16.5%)	Tava et al., 2010)
	−5.012	*C. rupestris s.l.*	germacrene D (42.3%)	
Jordan	−6.279	*C. damascena*	Fokienol (11.4%)	(Khleifat et al., 2019)
Spain	−6.253	*C. polymorpha Lag*	Heptacosane (11.5%)	(Formisano et al., 2006).
Croatia	−4.413	*C. grinensis Reuter*	p-Vinyl guaiacol (21.5%)	(Riccobono et al., 2017).
Bulgaria	−4.745	*C. apiculata Lebed*	Caryophyllene oxide (15.8%)	
Lebanon	−6.222	*C. eryngioides Lam*	Hexadecanoic acid (33.2%)	(Senatore et al., 2005).
	−6.125	*C. iberica Trev*	4-Vinyl guaiacol (8.5%)	
Greece	−6.523	*C. grisebachii subsp. Grisebachii*	6,10,14-Trimethyl-pentadecan-2-one (12.9%)	(Djeddi et al., 2011).
	−6.025	*C. affinis Friv.*	Tetracosane (7.8%)	
Ligands of Control				
BHT	−5.052			
EDTA	−5.591			
Ours Results				
L39	−7.184			
Analogue-1	−6.472			
Analogue-2	−6.564			
Analogue-3	−7.270			
Analogue-4	−7.697			
L42	−7.158			

3.2.2.2. Structural dynamics properties. We have studied the evolution structural dynamics of the best test compound, (Z)-phytol (Ligand 39) (See Table 5) by IMODS. Results of structural molecular dynamics simulation are listed in Figure S2 (Supplementary Materials).

The normal mode analysis (NMA) of the prepared, (Z)-phytol (Ligand 39)-*catalase* (*Cat*) complex was illustrated in (Figure S2a) From the molecular dynamics study of the prepared (Z)-phytol (Ligand 39)—*catalase* (*Cat*) complex, it was clear that the prepared enzyme-ligand complex had quite high eigenvalue of 1.927144e − 04 the eigenvalue is illustrated in Figure S2(b). However, the variance map showed a higher degree of cumulative variances than individual variances (Figure S2c). The elastic network map and co-variance also produced quite satisfactory results (Figure S2d and S2e respectively). The deformability graphs of the complex (Z)-phytol (Ligand 39)—*catalase* (*Cat*) illustrate the peaks in the graphs correspond to the regions in the protein with deformability (Figure S2f). The two selected ligand molecules can be used as potential agents to deplete DPPH and free radicals. Overall, in our study, (Z)-phytol (Ligand 39) emerged as the most potent anti-*catalase* (*Cat*) agent. However, more *in vitro* and *in vivo* researches should be performed on the (Z)-phytol (Ligand 39) the best ligands to confirm the findings of this study.

3.2.3. The OSIRIS property explorer and Bioisosteric replacement

A computational study was carried out for the best compounds to assess their **OSIRIS** properties. The obtained value is depicted in Table 9 and the results of predicted toxicity risks of other compounds are summarized in Table S8 (Supplementary Materials). Prediction results are valued and color coded (Nalini et al., 2011). The predicted results of **Bioisosteric replacement** are presented in Table 10.

The results summarized in Table 9 (Supplementary Materials Table S8) revealed that compounds L22, L23, L30, L33 and L39, L40, L42, L60 are the best ligands while L24, L36 have less affinity via the catalase target and L58 was predicted to cause irritation. Ligand L50 does not to possess druglikeness properties since it is predicted to be tumorigenic, mutagenic, irritant and moderately reproductive. Therefore, we are interested in the two compounds L39 and L42 with a remarkable interest in L39, because the former has good complementarity with the site of catalase and DNA sequence. Therefore, we thought to propose another molecule by using fragments of the compound-39. For this, we used, Molopt (A web server for drug design using bioisosteric transformation) which automatically generates analogs lists by replacing molecular substructures with chemical groups with similar biological properties. The resulting set of transforming analogs can be evaluated for future synthesis.

3.2.4. In silico assessment of the ADMET properties and drug-likeness

Poor pharmacokinetics Absorption, Distribution, Metabolism, Excretion and Toxicity (ADMET) is the major concern for the failure of drug candidates in clinical trials. So, knowing ADME features for the compound in advance is more important for drug discovery. The predicted results of drug-likeness,

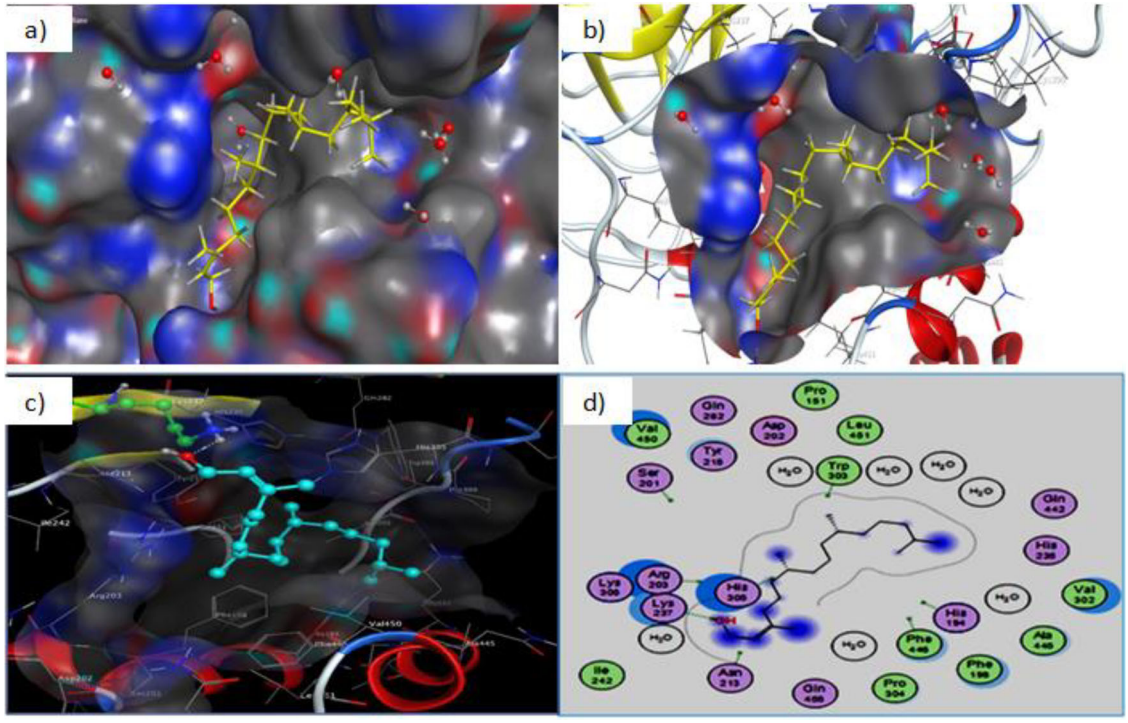

Figure 3. Displaying the Catalase binding site cavity 3D interaction diagram of (Z)-Phytol with pocket (b) and without pocket (c); Binding mode of (Z)-Phytol as 2D diagram (d). The binding patterns (Z)-Phytol in the active site of Catalase, in which (Z)-Phytol is appeared in stick model with pink while the surface of *Cat* is shown in blue red green (a).

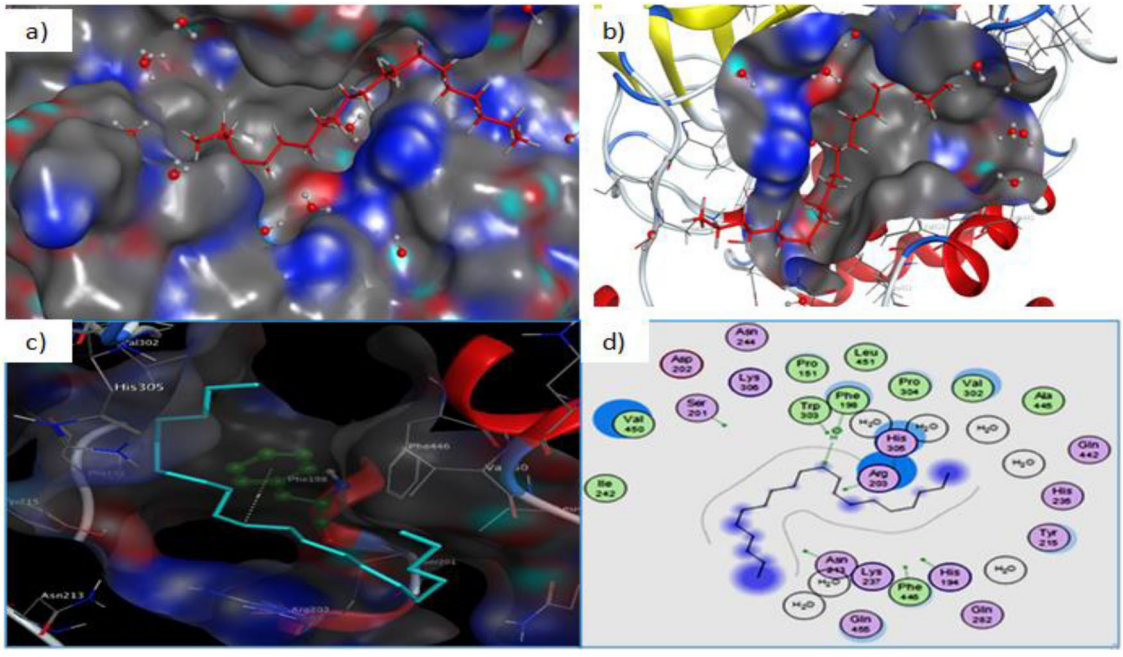

Figure 4. Displaying the Catalase binding site cavity 3D interaction diagram of Eicosane with pocket (b) and without pocket (c); Binding mode of Eicosane as 2D diagram (d). The binding patterns (Z)-Phytol in the active site of Catalase, in which Eicosane is appeared in stick model with pink while the surface of *Cat* is shown in blue red green (a).

pharmacokinetics and organ toxicity are presented in Tables 11, 12, and 13, respectively.

3.2.4.1. Drug-likeness evaluation. A good drug candidate is absorbed in required time and well distributed throughout the system for its effective metabolism and action. Table 11 depicts the drug-likeness properties of test compounds with least binding energies predicted using OSIRIS Property Explorer.

Result of Drug-likeness prediction and Physicochemical Properties (PC) for other compounds is listed in Tables S9 and S10 (Supplementary Materials) respectively.

The results listed in Table 11 revealed that ligand (Z)-phytol (Ligand 39), (E)-phytol (Ligand 60), eicosane (Ligand 42),

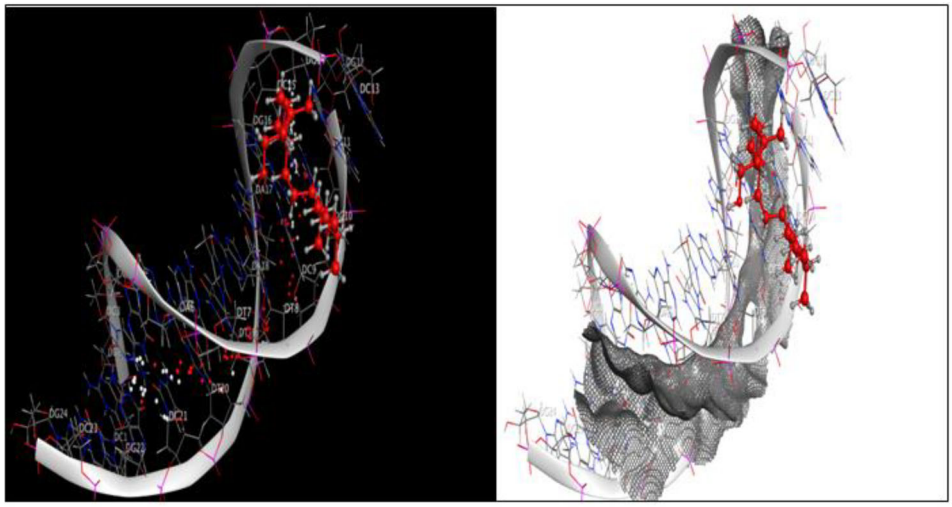

(a) Z-Phytol L39

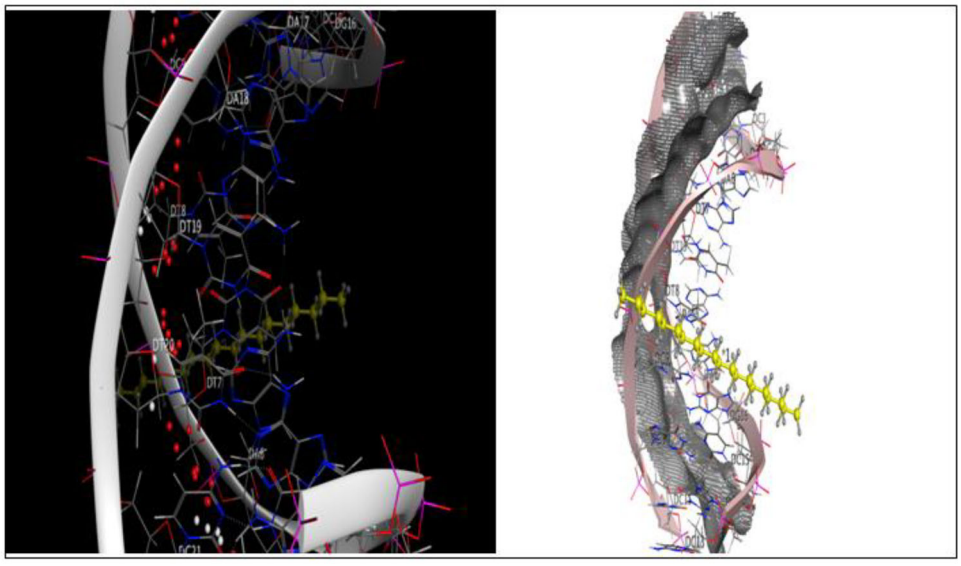

(b) Eicosane L42

Figure 5. Molecular docked model of the most favorable binding site of compounds (a) L39 and (b) L42 with DNA dodecamer duplex of sequence d (CGCGAATTCGCG)2 (PDB ID: 1BNA).

heneicosane (Ligand 40), have high absorption with a low molecular weight of order 296.54. Also, we can note that these compounds comply with Lipinski's rule of 5 Veber's rules and Egan's rule. MW range 264.41 (<500), A log *S* value indicates solubility; the lesser the log *S* value, the higher the solubility, which would enhance the absorption log for (Z)-phytol (Ligand 39) and eicosane (Ligand 42) were −4.63 and −5.84, respectively. A lower molecular weight would again enhance the absorption rate and thus most of the drugs were tried to be kept at the lowest possible molecular weight, suggesting that these compounds would not be expected to cause problems with oral bioavailability.

The ADME parameters were calculated for compounds under study, i.e. L22, L23, L30, L33, L39, L40, L42, and L60 by calculating the different Physico-chemical and bio-pharmaceutical highlights (Table 11; Supplementary Table S10).

The results indicated that the molecular refractivity was 69.04, 69.04, 70.46, 70.46, 80.48, 103.06, 98.25 and 98.94 for lead compounds, namely, L22, L23, L30, L33, L39, L40, L42, and L60, respectively. Water solubility properties were calculated through Log S ESOL Class (−3.56, −3.76, −3.29, −3.51, −5.98,−7.41, −7.05 and −5.98), log S AliClass (−3.70, −4.02, −3.49, −3.86, −8.47, −10.96, −10.40 and −8.47), SILISCOS-ITClass (−3.07, −3.32,−3.41, −3.21, −5.51, −8.34,−7.94 and −5.51) class. Lipophilicity is a key physicochemical property that plays a crucial role in determining ADMET (absorption, distribution, metabolism, excretion, and toxicity) properties and the overall suitability of drug candidates. The results were assessed for ILOGP and SILISCOS-IT which revealed that all compounds except (Z)-phytol (Ligand 39), (E)-phytol (Ligand 60), eicosane (Ligand 42), heneicosane (Ligand 40) (ILOGP4.78, 4.77, 5.64, 5.85 and SILISCOS-IT 6.57, 6.57, 7.98, 8.43), respectively showed a most favorable range, which describes a good balance between permeability and solubility and is expected to show good bioavailability upon oral drug administration. GI absorption predicted was low for each selected molecule. Drugs diffuse across a cell membrane in a concentration

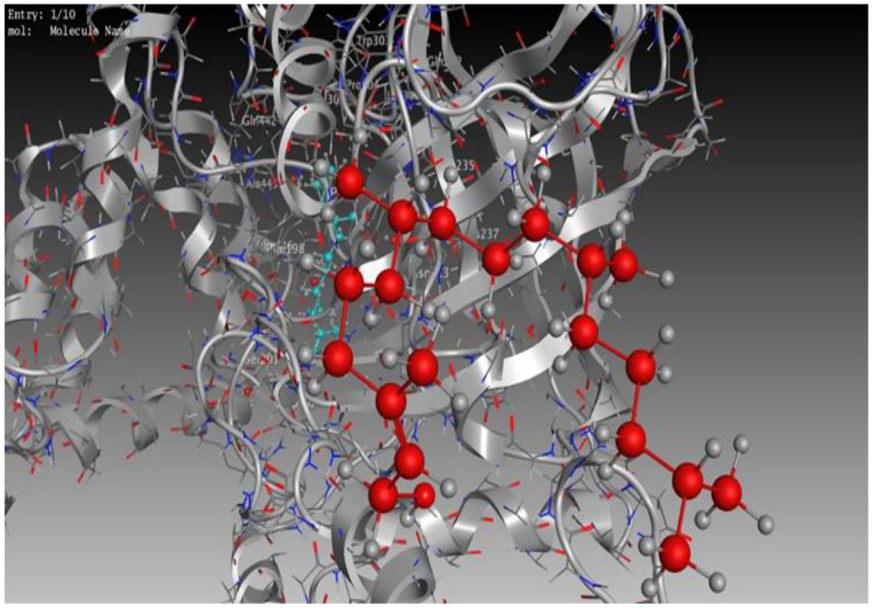

Figure 6. The compound—39; docked (blue) into the binding site of Cat the final ligand pose and the docking pose after a molecular dynamics (MD) in NVT simulation.

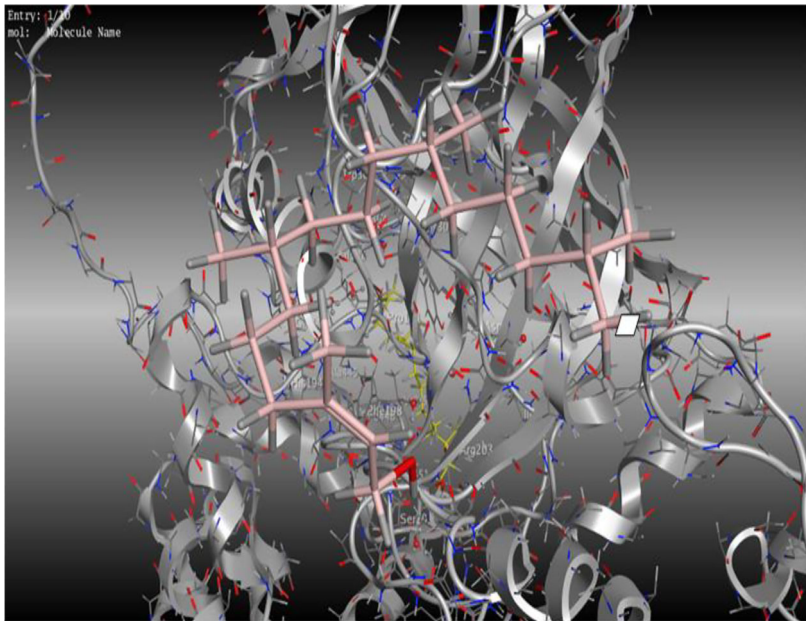

Figure 7. The compound—39; docked (yellow) into the binding site of Cat the final ligand pose and the docking pose after a molecular dynamics (MD) in NPT simulation.

gradient, a region of high concentration (e.g. gastrointestinal fluids) to a region of low concentration (e.g. blood). This permeability foresight helps to understand the outcomes of ADMET and the cell-based bioassays. The results showed that the permeability over human skin was found to be −4.71, −4.49, −5.25, −5.00, −2.29, −0.31, −0.60 and −2.29 cm/s for compounds viz., L22, L23, L30, L33, L39, L40, L42, and L60, respectively. These compounds showed almost no possibility to cross the BBB except L30 and L33. All medicines intended to work on the body pass into the blood stream. In this way, the fate of the drug—or rather its active ingredient—is commonly divided into four main stages: ADME (absorption, distribution in the body, metabolism and elimination) (See Table 12).

Apropos, the absorption parameters compound L39; and L42 presents a promising oral availability, due to the optimal Caco-2 cell permeability and HIA (>0.9 and Human intestinal >90%, respectively) (See Table 12).

3.2.4.2. ADME-T properties. Here, we evaluated the ADME properties of the selected L39–L42 and analogues compounds by using in silico SwissADME server to see the pharmacokinetic properties (Daina et al., 2017). The Absorption, Distribution, Metabolism, Excretion and Toxicity properties of the selected and analogues compounds have shown in Table 12.

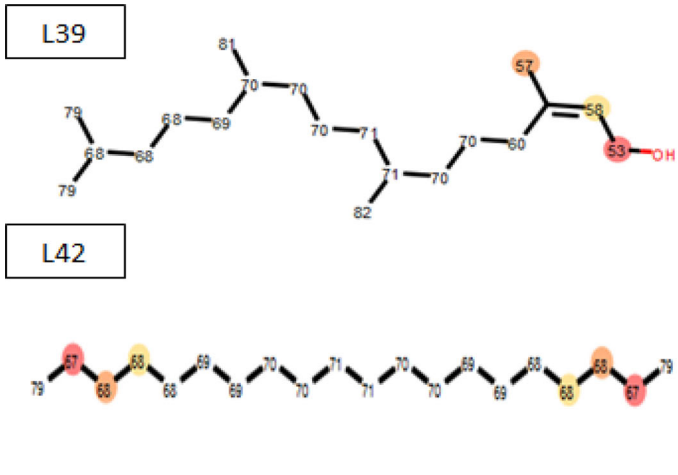

3A4 Ranking	Atom	3A4 Score	Energy	2DSASA
1	C.13	53.3	62.2	34.2
2	C.15	57.3	66.4	52.8
3	C.12	57.7	65.6	23.3

3A4 Ranking	Atom	3A4 Score	Energy	2DSASA
1	C.2	67.0	75.9	33.6
2	C.3	67.6	75.9	29.5
3	C.4	68.1	75.9	27.5

Figure 8. SMARTCyp results illustrating the metabolic sites for L39 and L42 which were predicted correctly with top-ranking atoms and ranked depending on the major metabolite.

All compounds passed the AMES tests. The volume of distribution (VDss) for our two best ligands (0.385 and 0.614 for L39 and L42, respectively) suggests that the drug will be distributed in the tissue as potent antioxidative agents. The control ligands, ethylenediaminetetraacetic acid (EDTA) and the Lref (NADPH) co-crystallized inhibitor are entirely unable to penetrate the central nervous system (CNS). The distribution and absorption parameters, respectively, have been graphically represented by the extended and renewed version of the Edan-Egg (Egg) model named Brain Or Intestinal EstimateD (BOILED) permeation predictive model (BOILED-Egg) (Figure S3, Supplementary Materials).

The graph (Figure S3, Supplementary Materials) showed that the ligands butyl hydroxyl toluene (BHT), β-eudesmol and Υ-eudesmol, analogue-1 and analogue-2 are absorbed by the brain. The ligands Z-phytol E-phytol, analogue-3 and analogue-4 showed gastrointestinal absorption within acceptable limits, except for ligands ethylenediaminetetraacetic acid (EDTA) and the Lref (NADPH) (TPSA 155.68 and 393.56 Å^2, respectively.

3.2.4.3. Prediction toxicity risk. Studying the toxicity profile was necessary in order to access the safety profile of the desired compounds. All results of toxicological pathways, including organ toxicity, toxicity and stress response pathways are given in Table 13. To identify the toxicity of the selected L39–L42, BHT, EDTA and analogues compounds, we used ProtoxII (Banerjee et al., 2018).

Organ Toxicity, Toxicity and Stress response pathways were also carried out for 10 biological activities. We note that butylated hydroxyltoluene (BHT) Predicted LD50 is 650 mg/kg and falls to Class 4 while 5000 mg/kg was Predicted for ethylene diaminetetraacetic and falls in class 2 of Toxicity Class. BHT falls to class 4 with range of 300 to 2000 mg/kg, these would be harmful in case of oral delivery. In addition, the compounds (Z)-phytol L39 was inactive for all toxic effects but eicosane L42 was active for androgen receptor (AR). (Z)-phytol L39 was in the toxicity class 5 and nontoxic, hence the best compound for our study. The toxicity class profile is in the order; (Z)-phytol L39 Predicted (Class: 5) >butyl hydroxyl toluene (BHT) (Class: 4 >eicosane) L42 (Class: 4>) ethylenediaminetetraacetic acid (EDTA) (Class: 2).

3.2.5. Pharmacophore mapping

Metabolism presents an essential function in the drug-drug interaction and bioavailability of drugs. Only the free form of the drug can bind with drug-metabolizing enzymes. To study the metabolic behavior of lead compounds, it is very important to study the cytochrome P450 enzymes (CYPs) as they are the most notable class of enzymes.

The possible sites of a chemical compound are illustrated by the circles on the chemical structure of the compound (Zaretzki et al., 2013). Figure 8 showed the possible interaction of L39 and L42 with CYP450 (3A4). So, the Site of Metabolism (SOM) at C1, C2, and C3 sites was predicted, and the ability of the two ligands to activate/inhibit the cytochrome system was determined.

The P450 SOM predictions showed that Z-phytol L39 had 4 sites of metabolism (SOMs) for the CYP450 1A2, 450 2A6 enzyme, CYP450 2B6, CYP450 2C8, CYP450 2C19, CYP450 2D6, CYP450 2E1 and CYP450 3A4 and 5 sites for CYP450 2C9. Are given in Table S11 (Supplementary Materials).

The Pharmacophore Mapping was carried out for the (Z)-phytol best ligand of the *oxygenated diterpene*. (Z)-phytol showed 1 Hydrogen acceptor bonds, 12 Hydrophobic groups, one Aromatic rings and 2 Hydrogen donor bonds. It also generated a good number of good contacts with the Pharmacophore of catalase, Figure 9.

The Pharmacophore of Z-phytol generates a hypothesis which can be applied successfully in biological screening for further experiments (Dixon et al., 2006).

Validation of our results, for essential oils of *C. sulphurea*, the synthetic antioxidant butyled hydroxyl toluene (BHT) and ethylenediaminetetraacetic acid (EDTA) and some species of *Inula* genuses are given in Table 14.

According to the table above, we note also that the compound L39 and their analogues have a high value of energy score compared to other compounds.

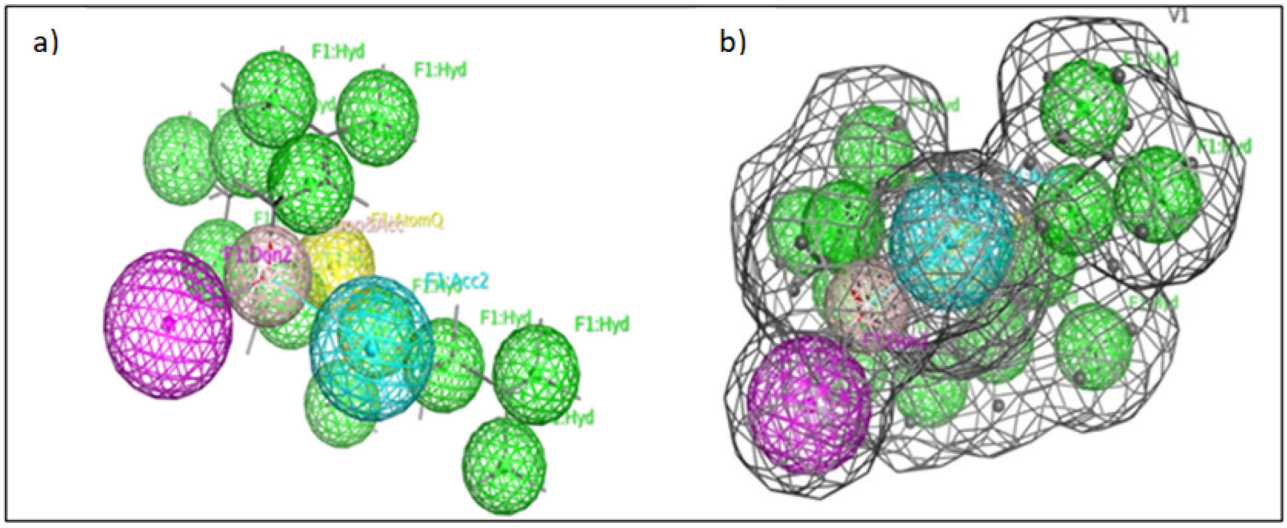

Figure 9. (a) Pharmacophore Mapping of Z-phytol L39. (b) Asteric constriction (dark gray) was added to the pharmacophore model.

The Oxygenated diterpene compounds were the most dominant. The complex formed by the compound L39 (Z)-phytol gives a low energy value of the score −7.148 kcal mol^{-1} that it is very close to the value of the clinical drugs (see Table 14), this compound establishes one interaction LYS 237 with the residues of active sites of the catalase (Figure 3).

The results presented in Table 11 revealed that compound L39 has high lipophilicity and high coefficient of skin permeability. Therefore, we propose (Z)-phytol was the best ligand which allows the inhibition of three targets and *ctDNA* sequence. So, we suggest (Z)-phytol present in **(**oxygenated diterpene) with its validated activity score (−7.184, −3.993, −4.413, −6.978); respectively for three targets and ctDNA sequence as a *new oral ligand*. According to its pharmacophore properties the compound 39 generated a hypothesis which can be applied successfully in biological screening for further experiments (Figure 9). *In vivo,* many studies were focused on the inhibitory effect of the sulphurea compounds, on key enzymes linked to investigate antioxidant activity; catalase and superoxide dismutase. The results of Souza et al. (2019) have proved that **extracts** of *C***. *sulphurea*** showed IC_{50} values of 103.9 at 24 and 48 h. Our results showed that essential oil *of C***. *sulphurea*** showed IC_{50} values of 2.06 g/L and 1.29 g/L. Through these results, we can conclude that, our oil presented an excellent antioxidant activity.

In our research the software platform that integrates visualization and modeling detect the hydrophobic interactions between (Z)-phytol (constituent molecules of the aerial and root parts of essential oil of ***C. sulphure***) and the three *endogenous enzymes*. The orientations of the docked ligands are consistent with a mechanism whereby these hydrophobic compounds dock into a hydrophobic pocket near the active site, there by blocking binding of the receptor. The results revealed inhibitory activities against novel three targets. Furthermore, compound-39 Z-phytol showed a high level of gastrointestinal adsorption, which contributes to good oral bioavailability. Consequently, the study carried out in this research reveals many secrets conveyed by the use of magic plants. At the end of our study, we propose that all biological activity depends on the presence of certain metabolites inside the tissues of the plant. The results obtained in this study reveal that (Z)-phytol and eicosane have potential antioxidant ability in three receptors via Reactive oxygen species (ROS) generation. Thus, (Z)-phytol and eicosane may be used for more analyses in order to further evaluate their efficiency in the reduction of oxidative stress and a possible antioxidant to be used in the pharmaceutical industry.

4. Conclusion

The present research aimed at the chemical and biological investigation of the essential oil of the aerial and root parts of the *C. sulphurea* species in hopes to find new natural products. The results showed that essential oil of *C. sulphurea* is a good source of caryophyllene oxide, aplotaxene and (Z)-phytol. The essential oils demonstrated greater antioxidant activity. However, no information was found in the available literature about the biological *in vivo* and *in vitro* activities of *C. sulphurea*. It would be interesting to study the antioxidant activity of these essential oils to check whether they possess antioxidant activities. The inhibition of Catalase receptor was theoretically investigated by two methods of computational chemistry: molecular docking analyses, MD simulations, ADME properties and pharmacological knowledge. The results reveal that ligand natural inhibitor (Z)-phytol L39 and eicosane L42 of essential oils from aerial and root parts of *C. sulphurea* during its vegetative cycle has an affinity to interact with cDNA sequence and three receptors. Compound (Z)-phytol L39 and their analogues showed better antioxidant, scavenging activity than other compounds. The results were also analysed computationally using the molecular dynamic and a molecular docking approach. From two analyses, it was also found that among all the tested compounds, compound 39 exhibited the best antioxidant activity. Moreover, the penetration through the Blood-Brain Barrier came out to be best for (Z)-phytol and their analogues than the control molecule and Lref. (Z)-phytol and their analogues were the best inhibitors for 1dgb, considering the pharmacokinetic

and pharmacodynamic properties. (Z)-phytol (Oxygenated diterpene) has the highest binding affinity among all the inhibitors, it is proposed as a *natural orally active* drug, and it may also be a good candidate for further biological and pharmacological investigations. The results reveal that (Z)-phytol L39 and their analogues have potential antioxidant ability in at least three *endogenous* receptors (*catalase (CAT), superoxide dismutase (SODs) and glutathione peroxidase (GPX)* and DNA sequence) via ROS generation. Thus, (Z)-phytol can be used as templates for further development of antioxidant therapeutic agents.

Acknowledgements

Authors thanks the Algerian Ministry of Higher Education and Scientific Research for the support under the PRFU project (approval no. B00L01UN130120190009) and (approval no. BOOL01UN130120180004).

Disclosure statement

The authors declare no conflict of interest.

Funding

The author(s) reported there is no funding associated with the work featured in this article.

References

Alam, M. N., Bristi, N. J., & Rafiquzzaman, M. (2013). Review on in vivo and in vitro methods evaluation of antioxidant activity. *Saudi Pharmaceutical Journal*, *21*(2), 143–152. https://doi.org/10.1016/j.jsps.2012.05.002

Alam, S., & Khan, F. (2018). Virtual screening, docking, ADMET and system pharmacology studies on garcinia caged xanthone derivatives for anticancer activity. *Scientific Reports*, *8*(1), 1–16. https://doi.org/10.1038/s41598-018-23768-7

AL-DALAEN, Said M. et AL-QTAITAT, Aiman I. (2014). Oxidative stress versus antioxidants. *American Journal of Bioscience and Bioengineering*, 2(5), 60. https://doi.org/10.11648/j.bio.20140205.11

Agbadah, E. E., Nwachukwu, K. C., & Okoh, M. P. (2016). Biochemical effects of ethylene diamine tetra-acetic acid (EDTA) on cadmium treated maize (*Zea mays* L.) and cowpea (*Vigna unguiculata* L.). *African Journal of Biotechnology*, *15*(15), 593–600.

Ayromlou, A., Masoudi, S., & Mirzaie, A. (2020). Chemical composition, antioxidant, antibacterial, and anticancer activities of *Scorzoneracalyculata*boiss. and *Centaurea irritans*wagenitz. Extracts, endemic to iran. *Journal of Reports in Pharmaceutical Sciences*, *9*(1), 118.

Atika Eddaikra and Naouel Eddaikra (2021). *Endogenous Enzymatic Antioxidant Defense and Pathologies*.In Antioxidants.IntechOpen. https://doi.org/10.5772/intechopen.95504

Banerjee, P., Eckert, A. O., Schrey, A. K., & Preissner, R. (2018). ProTox-II: A webserver for the prediction of toxicity of chemicals. *Nucleic Acids Research*, *46*(W1), W257–W263.

Bekhechi, C., Boti, J. B., Bekkara, F. A., Abdelouahid, D. E., Casanova, J., & Tomi, F. (2010). Isothymol in Ajowan essential oil. *Natural Product Communications*, *5*(7), 1934578X1000500. https://doi.org/10.1177/1934578X1000500726

Belabbes, R., Dib, M. E. A., Djabou, N., Ilias, F., Tabti, B., Costa, J., & Muselli, A. (2017). Chemical variability, antioxidant and antifungal activities of essential oils and hydrosol extract of *Calendula arvensis* L. from western Algeria. *Chemistry & Biodiversity*, *14*(5), e1600482. https://doi.org/10.1002/cbdv.201600482

Belkassam, A., Zellagui, A., Gherraf, N., Flamini, G., Cioni, P. L., Rebbas, K., & Smaili, T. (2019). Assessment of Antioxidant effect of the essential oil and methanol extract of *Centaurea dimorpha* Viv.aerial parts from Algeria. *Acta Scientifica Naturalis*, *6*(1), 54–62. https://doi.org/10.2478/asn-2019-0008

Bereksi, M. S., Hassaïne, H., Bekhechi, C., & Abdelouahid, D. E. (2018). Evaluation of antibacterial activity of some medicinal plants extracts commonly used in Algerian traditional medicine against some pathogenic bacteria. *Pharmacognosy Journal*, *10*(3), 507–512. https://doi.org/10.5530/pj.2018.3.83

Bissantz, C., Kuhn, B., & Stahl, M. (2010). A medicinal chemist's guide to molecular interactions. *Journal of Medicinal Chemistry*, *53*(14), 5061–5084. https://doi.org/10.1021/jm100112j.

Birben, E., Sahiner, U. M., Sackesen, C., Erzurum, S., & Kalayci, O. (2012). Oxidative stress and antioxidant defense. *The World Allergy Organization Journal*, *5*(1), 9–19. https://doi.org/10.1097/WOX.0b013e3182439613

Blois, M. S. (1958). Antioxidant determinations by the use of a stable free radical. *Nature*, *181*(4617), 1199–1200. https://doi.org/10.1038/1811199a0

Bouyanzer, A., Majidi, L., & Hammouti, B. (2006). Effect of eucalyptus oil on the corrosion of steel in 1M HCl. *Bulletin of Electrochemistry*, *22*(7), 321–324.

Branen, A. L., Richardson, T., Goel, M. C., & Allen, J. R. (1973). Lipid and enzyme changes in the blood and liver of monkeys given butylated hydroxytoluene and butylated hydroxyanisole. *Food and Cosmetics Toxicology*, *11*(5), 797–806.

Brünger, A., Brooks, C. L., III, & Karplus, M. (1984). Stochastic boundary conditions for molecular dynamics simulations of ST2 water. *Chemical Physics Letters*, *105*(5), 495–500. https://doi.org/10.1016/0009-2614(84)80098-6

Chen, K. C., Chen, H. Y., & Chen, C. Y. C. (2014). Potential protein phosphatase 2A agents from traditional Chinese medicine against cancer. *Evidence-Based Complementary and Alternative Medicine: eCAM*, *2014*, 436863–436863. https://doi.org/10.1155/2014/436863

Chen, Y. C. (2015). Beware of docking!. *Trends in Pharmacological Sciences*, 36(2), 78–95. https://doi.org/10.1016/j.tips.2014.12.001

Cheng, F., Li, W., Zhou, Y., Shen, J., Wu, Z., Liu, G., & Tang, Y. (2012). admetSAR: A comprehensive source and free tool for assessment of chemical ADMET properties. *J. Chem. Inf. Model.*, *52*(11), 3099–3105. https://doi.org/10.1021/ci300367a

Chenafa, H., Mesli, F., Daoud, I., Achiri, R., Ghalem, S., & Neghra, A. (2021). In silico design of enzyme α-amylase and α-glucosidase inhibitors using molecular docking, molecular dynamic, conceptual DFT investigation and pharmacophore modelling. *Journal of Biomolecular Structure and Dynamics*, *39*, 1–22. https://doi.org/10.1080/07391102.2021.1882340

Clément, G., &Slenzka, K. (Eds.). (2006). *Fundamentals of space biology: Research on cells, animals, and plants in space* (Vol. 18). Springer Science & Business Media.

Conseil de l'Europe. (1996). Pharmacopée européenne.

Cross, J. B., Thompson, D. C., Rai, B. K., Baber, J. C., Fan, K. Y., Hu, Y., & Humblet, C. (2009). Comparison of several molecular docking programs: Pose prediction and virtual screening accuracy. *Journal of Chemical Information and Modeling*, *49*(6), 1455–1474. https://doi.org/10.1021/ci900056c

Daina, A., Michielin, O., & Zoete, V. (2017). SwissADME: A free web tool to evaluate pharmacokinetics, drug-likeness and medicinal chemistry friendliness of small molecules. *Scientific Reports*, *7*(1), 42717–42713. https://doi.org/10.1038/srep42717

Daoud, I., Melkemi, N., Salah, T., & Ghalem, S. (2018). Combined QSAR, molecular docking and molecular dynamics study on new Acetylcholinesterase and Butyrylcholinesterase inhibitors. *Computational Biology and Chemistry*, *74*, 304–326. https://doi.org/10.1016/j.compbiolchem.2018.03.021

Didierjean, C., & Tête-Favier, F. (2016). Introduction to protein science. Architecture, function and genomics. By Arthur M. Lesk 2016. Pp. 466 Paperback. Price GBP 39.99. ISBN 9780198716846.Acta Crystallographica Section D: Structural Biology, 72(12), 1308–1309.

Dixon, S. L., Smondyrev, A. M., Knoll, E. H., Rao, S. N., Shaw, D. E., & Friesner, R. A. (2006). PHASE: A new engine for pharmacophore perception, 3D QSAR model development, and 3D database screening: 1.

Methodology and preliminary results. *Journal of Computer-Aided Molecular Design*, *20*(10–11), 647–671.

Djeddi, S., Sokovic, M., & Skaltsa, H. (2011). Analysis of the essential oils of some Centaurea species (Asteraceae) growing wild in Algeria and Greece and investigation of their antimicrobial activities. *Journal of Essential Oil Bearing Plants*, *14*(6), 658–666. https://doi.org/10.1080/0972060X.2011.10643986

DREW, Horace R., WING, Richard M., TAKANO, Tsunehiro, et al. (1981). Structure of a B-DNA dodecamer: conformation and dynamics. *Proceedings of the National Academy of Sciences*, 78(4), 2179–2183. https://doi.org/10.1073/pnas.78.4.2179

Eddaikra, A., & Eddaikra, N. (2021). Endogenous enzymatic antioxidant defense and pathologies. In *Antioxidants*. IntechOpen.

Erdogan, T., Sumer, B., Ozcı nar, O., Cakilcioglu, U., Demirci, B., Baser, K. H. C., & Kivcak, B. (2017). Essential oil composition of three Centaurea Species from Turkey: Centaurea aggregata Fisch. & Mey.ex. DC. subsp. aggregata, C. balsamita Lam. and C. behen L. *Records of Natural Products*, *11*(1), 69.

Figueiredo, P. L. B., Pinto, L. C., da Costa, J. S., da Silva, A. R. C., Mourão, R. H. V., Montenegro, R. C., da Silva, J. K. R., & Maia, J. G. S. (2019). Composition, antioxidant capacity and cytotoxic activity of *Eugenia uniflora* L. chemotype-oils from the Amazon. *Journal of Ethnopharmacology*, *232*, 30–38.

Firouznia, A., Akbari, M. T., Rustaiyan, A., Masoudi, S., Bigdeli, M., & Anaraki, M. T. (2007). Composition of the essential oils of *Artemisia turanica* Krasch., *Helichrysum oocephalum* Boiss. and *Centaurea ispahanica* Boiss. three asteraceae herbs growing wild in Iran. *Journal of Essential Oil Bearing Plants*, *10*(2), 88–93. https://doi.org/10.1080/0972060X.2007.10643524

Formisano, C., Senatore, F., Bellone, G., Bruno, M., Grassia, A., Raio, A., & Rigano, D. (2006). Chemical composition and biological activity of essential oil from flowerheads of *Centaurea polymorpha* Lag. (Asteraceae) growing wild in Spain. *Polish Journal of Chemistry*, *80*(4), 617–622.

Francisco, A. (1995). JB HARBORNE (ED.) *The flavonoids–Advances in research since* 1986 Chapman & Hall, London, 676 pp. ISBN 0-412-48070-0. https://doi.org/10.1002/pca.2800060109

Çam, M., Hışıl, Y., & Durmaz, G. (2009). Classification of eight pomegranate juices based on antioxidant capacity measured by four methods. *Food Chemistry*, *112*(3), 721–726. https://doi.org/10.1016/j.foodchem.2008.06.009

Geronikaki, A., Poroikov, V., Hadjipavlou-Litina, D., Filimonov, D., Lagunin, A., & Mgonzo, R. (1999). Computer aided predicting the biological activity spectra and experimental testing of new thiazole derivatives. *Quantitive Structure-Activity Relationships*, *18*(1), 16–25. https://doi.org/10.1002/(SICI)1521-3838(199901)18:1<16::AID-QSAR16>3.0.CO;2-O

Greenstein, J. P., & Andervont, H. B. (1943). Note on the liver catalase activity of pregnant mice and of mice bearing growing embryonic implants. *Journal of the National Cancer Institute*, *4*(3), 283–284.

Halgren, T. A. (1996). Merck molecular force field. I. Basis, form, scope, parameterization, and performance of MMFF94. *Journal of Computational Chemistry*, *17*(5–6), 490–519. https://doi.org/10.1002/(SICI)1096-987X(199604)17:5/6<490::AID-JCC1>3.0.CO;2-P

Halgren, T. A. (1999). MMFF VII. Characterization of MMFF94, MMFF94s, and other widely available force fields for conformational energies and for intermolecular-interaction energies and geometries. *Journal of Computational Chemistry*, *20*(7), 730–748. https://doi.org/10.1002/(SICI)1096-987X(199905)20:7<730::AID-JCC8>3.0.CO;2-T

Hung, T. C., Lee, W. Y., Chen, K. B., Chan, Y. C., Lee, C. C., & Chen, C. Y. C. (2014). In silico investigation of traditional Chinese medicine compounds to inhibit human histone deacetylase 2 for patients with Alzheimer's disease. *BioMed Research International*, *2014*, 769867–769867. https://doi.org/10.1155/2014/769867

HyperChem v8. (2009). *Molecular modelling system*. Hypercube Inc.

Ighodaro, O. M., & Akinloye, O. A. (2018). First line defence antioxidants-superoxide dismutase (SOD), catalase (CAT) and glutathione peroxidase (GPX): Their fundamental role in the entire antioxidant defence grid. *Alexandria journal of medicine*, 54(4), 287–293. https://doi.org/10.1016/j.ajme.2017.09.001

Jennigs, W., & Shibamoto, T. (1980). *Qualitative analysis of flavor and fragrance volatiles by glass capillary gas chromatography. 465 Seiten*. Academic Press, New York, London, Sydney, Toronto, San Francisco 1980. https://doi.org/10.1002/food.19820260943

Jorgensen, W. L., Maxwell, D. S., & Tirado-Rives, J. (1996). Development and testing of the OPLS all-atom force field on conformational energetics and properties of organic liquids. *Journal of the American Chemical Society*, *118*(45), 11225–11236. https://doi.org/10.1021/ja9621760

Kabouche, A., Kabouche, Z., Touzani, R., & Bruneau, C. (2011). Flavonoids from *Centaurea sulphurea*. *Chemistry of Natural Compounds*, *46*(6), 966–967. https://doi.org/10.1007/s10600-011-9798-3

Kargı oğlu, M., Cenkci, S., Serteser, A., Konuk, M., & Vural, G. (2010). Traditional uses of wild plants in the middle Aegean region of Turkey. *Human Ecology*, *38*(3), 429–450. https://doi.org/10.1007/s10745-010-9318-2

Khleifat, K. M., Matar, S. A., Jaafreh, M., Qaralleh, H., Al-limoun, M. O., & Alsharafa, K. Y. (2019). Essential oil of Centaurea damascena aerial parts, antibacterial and synergistic effect. *Journal of Essential Oil Bearing Plants*, *22*(2), 356–367. https://doi.org/10.1080/0972060X.2019.1626292

KIM, Nam-Sun et LEE, Dong-Sun. (2004). Headspace solid-phase microextraction for characterization of fragrances of lemon verbena (Aloysia triphylla) by gas chromatography-mass spectrometry. *Journal of separation science*, 27(1-2), 96–100. https://doi.org/10.1002/jssc.200301603.

König, W. A., Joulain, D., & Hochmuth, D. H. (2001). Terpenoids and related constituents of essential oils. *Library of MassFinder*, *2.1*. Hamburg: Institute of Organic Chemistry. .

Kumar, R., Prakash, O., Pant, A. K., Isidorov, V. A., & Mathela, C. S. (2012). Chemical composition, antioxidant and myorelaxant activity of essential oils of *Globba sessiliflora* Sims. *Journal of Essential Oil Research*, *24*(4), 385–391. https://doi.org/10.1080/10412905.2012.692915

Kumarasamy, Y., Nahar, L., Cox, P. J., Dinan, L. N., Ferguson, C. A., Finnie, D. A., Jaspars, M., & Sarker, S. D. (2003). Biological activity of lignans from the seeds of *Centaurea scabiosa*. *Pharmaceutical Biology*, *41*(3), 203–206. https://doi.org/10.1076/phbi.41.3.203.15099

Lakhal, H., Boudiar, T., Kabouche, A., Kabouche, Z., Touzani, R., & Bruneau, C. (2010). New sesquiterpene lactone and other constituents from *Centaurea sulphurea* (Asteraceae). *Natural Product Communications*, *5*(6), 1934578X1000500. https://doi.org/10.1177/1934578X1000500603

Lanigan, R. S., & Yamarik, T. A. (2002). Final report on the safety assessment of BHT(1). *International Journal of Toxicology*, *21*(Suppl 2), 19–94.

Lipinski, C. A., Lombardo, F., Dominy, B. W., & Feeney, P. J. (1997). Experimental and computational approaches to estimate solubility and permeability in drug discovery and development settings. *Advanced Drug Delivery Reviews*, *23*(1–3), 3–25. https://doi.org/10.1016/j.addr.2012.09.019

Madkour, L. H. (2020). *Reactive oxygen species (ROS), nanoparticles, and endoplasmic reticulum (er) stress-induced cell death mechanisms*. Academic Press.

Mahoney, J. R., & Graf, E. (1986). Citric acid and EDTA as oxidant in a model system. *Journal of Food Science*, *51*(5), 1293–1296. https://doi.org/10.1111/j.1365-2621.1986.tb13108.x

Manjula, R., Wright, G. S., Strange, R. W., & Padmanabhan, B. (2018). Assessment of ligand binding at a site relevant to SOD 1 oxidation and aggregation. *FEBS Letters*, *592*(10), 1725–1737. https://doi.org/10.1002/1873-3468.13055

McLafferty, F. W., & Stauffer, D. B. (1994). Bench-top/PBM Mass spectrometry library search system, version 3.10 d. In *Wiley registry of mass spectral data*. Newfield: Palisade.

Medbouhi, A., Merad, N., Khadir, A., Bendahou, M., Djabou, N., Costa, J., & Muselli, A. (2018). Chemical composition and biological investigations of *Eryngium triquetrum* essential oil from Algeria. *Chemistry & Biodiversity*, *15*(1), e1700343. https://doi.org/10.1002/cbdv.201700343

Mesli, F., Daoud, I., & Ghalem, S. (2019). Antidiabetic activity of Nigella sativa (BLACK SEED)-by molecular modeling elucidation, molecular dynamic, and conceptual DFT investigation. *Pharmacophore*, *17868*(136.2380), C10H16.

Mesli, F., Ghalem, M., Daoud, I., & Ghalem, S. (2021). Potential inhibitors of angiotensin converting enzyme 2 receptor of COVID-19 by *Corchorus olitorius* Linn using docking, molecular dynamics, conceptual DFT investigation and pharmacophore mapping. *Journal of Biomolecular Structure and Dynamics*, *39*, 1–13. https://doi.org/10.1080/07391102.2021.1896389

Mesli, F., Medjahed, K., & Ghalem, S. (2013). Prediction of structural and thermodynamic properties of three products: 1-bromobenzene, tetrachlorethylene and 4-hydroxy-chromen-2-one using numerical methods. *Research on Chemical Intermediates*, *39*(4), 1877–1895. https://doi.org/10.1007/s11164-012-0722-7

Molecular Operating Environment (MOE). (2019). 2013.08; Chemical Computing Group Inc., 1010 Sherbooke St. West, Suite #910, Montreal, QC, Canada, H3A 2R7.

Naeim, H., El-Hawiet, A., Rahman, R. A. A., Hussein, A., El Demellawy, M. A., & Embaby, A. M. (2020). Antibacterial activity of *Centaurea pumilio* L. root and aerial part extracts against some multidrug resistant bacteria. *BMC Complementary Medicine and Therapies*, *20*(1), 1–13. https://doi.org/10.1186/s12906-020-2876-y

Nafis, A., Kasrati, A., Jamali, C. A., Mezrioui, N., Setzer, W., Abbad, A., & Hassani, L. (2019). Antioxidant activity and evidence for synergism of *Cannabis sativa* (L.) essential oil with antimicrobial standards. *Industrial Crops and Products*, *137*, 396–400. https://doi.org/10.1016/j.indcrop.2019.05.032

Najjar, F. M., Ghadari, R., Yousefi, R., Safari, N., Sheikhhasani, V., Sheibani, N., & Moosavi-Movahedi, A. A. (2017). Studies to reveal the nature of interactions between catalase and curcumin using computational methods and optical techniques. *International Journal of Biological Macromolecules*, *95*, 550–556.

Nalini, C. N., Deepthi, S. R., Ramalakshmi, N., & Uma, G. (2011). Toxicity risk assesment of isatins. *Rasayan Journal of Chemistry*, *4*(4), 829–833.

National Institute of Standards and Technology. (1999). PC version 1.7 of the NIST/EPA/NIH Mass spectral library.

Noguchi, N., & Niki, E. (1999). Chemistry of active oxygen species and antioxidants. *Antioxidant status, diet, nutrition, and health*., p. 20. https://doi.org/10.1201/9780367811099-1

Oke, F., Aslim, B., Ozturk, S., & Altundag, S. (2009). Essential oil composition, antimicrobial and antioxidant activities of *Saturejacuneifolia* Ten. *Food Chemistry*, *112*(4), 874–879. https://doi.org/10.1016/j.foodchem.2008.06.061

Oury, T. D., Day, B. J., & Crapo, J. D. (1996). Extracellular superoxide dismutase: A regulator of nitric oxide bioavailability. *Laboratory Investigation; a Journal of Technical Methods and Pathology*, *75*(5), 617–636.

Pal, S., Dey, S. K., & Saha, C. (2014). Inhibition of catalase by tea catechins in free and cellular state: A biophysical approach. *PLoS One*, *9*(7), e102460.

Panagouleas, C., Skaltsa, H., Lazari, D., Skaltsounis, A. L., & Sokovic, M. (2003). Antifungal activity of secondary metabolites of *Centaurea raphanina* ssp. *mixta,* growing wild in Greece. *Pharmaceutical Biology*, *41*(4), 266–270. https://doi.org/10.1076/phbi.41.4.266.15664

Parki, A., Chaubey, P., Prakash, O., Kumar, R., & Pant, A. K. (2017). Seasonal variation in essential oil compositions and antioxidant properties of Acorus Calamus L. accessions. *Medicines*, *4*(4), 81.

Parr, R. G., & Yang, W. (1989). *Density functional theory of atoms and molecules* (Vol. 1). Oxford University Press.

Putnam, C. D., Arvai, A. S., Bourne, Y., & Tainer, J. A. (2000). Active and inhibited human catalase structures: Ligand and NADPH binding and catalytic mechanism. *Journal of Molecular Biology*, *296*(1), 295–309.

Release, S. (2018). *2: Maestro, version 11.8*. Schrödinger, LLC.

Riccobono, L., Maggio, A., Bruno, M., Bancheva, S., Santucci, O., & Senatore, F. (2017). Chemical composition of the essential oil of *Centaurea grinensis* Reuter and *Centaurea apiculata* Ledeb: Growing wild in Croatia and Bulgaria, respectively and PCA analysis of subgenus Lopholoma (Cass.) Dobrocz. *Plant Biosystems*, *151*(6), 1035–1044. https://doi.org/10.1080/11263504.2016.1219419

Robert G. Parr and Yang Weitao. (1989). Density functional theory of atoms and molecules. *O xford University Press*, 1. https://doi.org/10.1093/oso/9780195092769.001.0001

Rodil, R., Quintana, J. B., & Cela, R. (2012). Oxidation of synthetic phenolic antioxidants during water chlorination. *Journal of Hazardous Materials*, *199–200*, 73–81. https://doi.org/10.1016/j.jhazmat.2011.10.058

Ruiz-Carmona, S., Alvarez-Garcia, D., Foloppe, N., Garmendia-Doval, A. B., Juhos, S., Schmidtke, P., Barril, X., Hubbard, R. E., & Morley, S. D. (2014). rDock: A fast, versatile and open-source program for docking ligands to proteins and nucleic acids. *PLoS Computational Biology*, *10*(4), e1003571.

Sangwan, N. S., Farooqi, A. H. A., Shabih, F., & Sangwan, R. S. (2001). Regulation of essential oil production in plants. *Plant Growth Regulation*, *34*(1), 3–21. https://doi.org/10.1023/A:1013386921596

Sarikurkcu, C., Ozer, M. S., Calli, N., & Popović-Djordjević, J. (2018). Essential oil composition and antioxidant activity of endemic *Marrubium parviflorum* subsp. *oligodon*. *Industrial Crops and Products*, *119*, 209–213. https://doi.org/10.1016/j.indcrop.2018.04.023

Sarwar, M. G., Dragisic, B., Salsberg, L. J., Gouliaras, C., & Taylor, M. S. (2010). Thermodynamics of halogen bonding in solution: Substituent, structural, and solvent effects. *Journal of the American Chemical Society*, *132*(5), 1646–1653. https://doi.org/10.1021/ja9086352

Sarwar, M. G., Ajami, D., Theodorakopoulos, G., Petsalakis, I. D., & Rebek, J. (2013). Amplified halogen bonding in a small space. *Journal of the American Chemical Society*, *135*(37), 13672–13675. https://doi.org/10.1021/ja407815t

Secilla, F. M., Rojas, J. A. G., & Devesa, J. A. (2012). *Centaurea sulphurea* Willd. (Asteraceae), novedad para la flora de *Andalucía occidental*. *Centaurea sulphurea* Willd. (Asteraceae), a novelty for the Western Andalusian flora. *Acta BotanicaMalacitana*, *37*, 233–234.

Sen, A., Kurkcuoglu, M., Yildirim, A., Senkardes, I., Bitis, L., & Baser, K. H. C. (2021). Chemical composition, antiradical, and enzyme inhibitory potential of essential oil obtained from aerial part of Centaurea pterocaula Trautv. *Journal of Essential Oil Research*, *33*(1), 44–52. https://doi.org/10.1080/10412905.2020.1839585

Senatore, F., Arnold, N. A., & Bruno, M. (2005). Volatile components of *Centaurea eryngioides* Lam. and Centaurea iberica Trev.var. hermonis Boiss. Lam., two Asteraceae growing wild in Lebanon. *Natural Product Research*, *19*(8), 749–754. https://doi.org/10.1080/14786410412331302136

Souza, J. M., Candido, A. C. B. B., & Pagotti, M. C. (2019). In vitro evaluation of the leishmanicidal potential of selected plant-derived extracts against Leishmania (Leishmania) amazonensis. *International Journal of Complementary & Alternative Medicine*, *12*(1), 36–41.

STANKOVIC, Milan. (2020).*Medicinal Plants and Natural Product Research*. MDPI-Multidisciplinary Digital Publishing Institute. Pages: 231. https://doi.org/10.3390/books978-3-03928-119-0

Stewart, James. J. P. (2007). Optimization of parameters for semi-empirical methods V: Modification of NDDO approximations and application to 70 elements. *Journal of Molecular Modeling*, 13(12), 1173–1213. https://doi.org/10.1007/s00894-007-0233-4

Stitou, M., Toufik, H., Bouachrine, M., & Lamchouri, F. (2021). Quantitative structure–activity relationships analysis, homology modeling, docking and molecular dynamics studies of triterpenoid saponins as Kirsten rat sarcoma inhibitors. *Journal of Biomolecular Structure and Dynamics*, *39*(1), 119–152. https://doi.org/10.1080/07391102.2019.1707122

Tars, K., Olin, B., & Mannervik, B. (2010). Structural basis for featuring of steroid isomerase activity in alpha class glutathione transferases. *Journal of Molecular Biology*, *397*(1), 332–340.

Tava, A., Esposti, S., Boracchia, M., & Viegi, L. (2010). Volatile constituents of *Centaurea paniculata* subsp. *carueliana* and *C. rupestris*sl (Asteraceae) from Mt. Ferrato (Tuscany, Italy). *Journal of Essential Oil Research*, *22*(3), 223–227. https://doi.org/10.1080/10412905.2010.9700308

Toda, M., Kubo, R., Saitō, N., & Hashitsume, N. (1991). *Statistical physics II: Nonequilibrium statistical mechanics* (Vol. 2). Springer Science & Business Media.

THOMSEN, René et CHRISTENSEN, Mikael H. (2006). MolDock: A new technique for high-accuracy molecular docking. *Journal of Medicinal Chemistry*, 49(11), 3315–3321. https://doi.org/10.1021/jm051197e

Trease, G.E. and Evans, W.C. (1983) *Textbook of pharmacognosy*. 12th Edition, Tindall and Co., London, 343–383.

Vyas, V., Jain, A., Jain, A., & Gupta, A. (2008). Virtual screening: A fast tool for drug design. *Scientia Pharmaceutica*, *76*(3), 333–360. https://doi.org/10.3797/scipharm.0803-03

Wang, H., Gao, X. D., Zhou, G. C., Cai, L., & Yao, W. B. (2008). In vitro and in vivo antioxidant activity of aqueous extract from *Choerospondiasaxillaris* fruit. *Food Chemistry*, *106*(3), 888–895. https://doi.org/10.1016/j.foodchem.2007.05.068

Wang, W., & Skeel, R. D. (2003). Analysis of a few numerical integration methods for the Langevin equation. *Molecular Physics*, *101*(14), 2149–2156. https://doi.org/10.1080/0026897031000135825

Yang, L., Zheng, X. L., Sun, H., Zhong, Y. J., Wang, Q., He, H. N., Shi, X. W., Zhou, B., Li, J. K., Lin, Y., Zhang, L., & Wang, X. (2011). Catalase suppression-mediated H_2O_2 accumulation in cancer cells by wogonin effectively blocks tumor necrosis factor-induced NF-κB activation and sensitizes apoptosis. *Cancer Science*, *102*(4), 870–876. https://doi.org/10.1111/j.1349-7006.2011.01874.x

Zaretzki, J., Bergeron, C., Huang, T. W., Rydberg, P., Swamidass, S. J., & Breneman, C. M. (2013). RS-WebPredictor: A server for predicting CYP-mediated sites of metabolism on drug-like molecules. *Bioinformatics (Oxford, England)*, *29*(4), 497–498. https://doi.org/10.1093/bioinformatics/bts705

Zatla, A. T., Dib, M. E. A., Djabou, N., Tabti, B., Meliani, N., Costa, J., & Muselli, A. (2017). Chemical variability of essential oil of *Daucus carota* subsp. *sativus* from algeria. *Journal of Herbs, Spices & Medicinal Plants*, *23*(3), 216–230. https://doi.org/10.1080/10496475.2017.1296053